

International Journal of Engineering (IJE)

ISSN : 1985-2312



VOLUME 4, ISSUE 3

PUBLICATION FREQUENCY: 6 ISSUES PER YEAR

International Journal of Engineering (IJE)

Volume 4, Issue 3, 2010

Edited By
Computer Science Journals
www.cscjournals.org

Editor in Chief Dr. Kouroush Jenab

International Journal of Engineering (IJE)

Book: 2010 Volume 4, Issue 3

Publishing Date: 31-07-2010

Proceedings

ISSN (Online): 1985-2312

This work is subjected to copyright. All rights are reserved whether the whole or part of the material is concerned, specifically the rights of translation, reprinting, re-use of illustrations, recitation, broadcasting, reproduction on microfilms or in any other way, and storage in data banks. Duplication of this publication of parts thereof is permitted only under the provision of the copyright law 1965, in its current version, and permission of use must always be obtained from CSC Publishers. Violations are liable to prosecution under the copyright law.

IJE Journal is a part of CSC Publishers

<http://www.cscjournals.org>

© IJE Journal

Published in Malaysia

Typesetting: Camera-ready by author, data conversion by CSC Publishing Services – CSC Journals, Malaysia

CSC Publishers

Editorial Preface

This is the third issue of volume four of International Journal of Engineering (IJE). The Journal is published bi-monthly, with papers being peer reviewed to high international standards. The International Journal of Engineering is not limited to a specific aspect of engineering but it is devoted to the publication of high quality papers on all division of engineering in general. IJE intends to disseminate knowledge in the various disciplines of the engineering field from theoretical, practical and analytical research to physical implications and theoretical or quantitative discussion intended for academic and industrial progress. In order to position IJE as one of the good journal on engineering sciences, a group of highly valuable scholars are serving on the editorial board. The International Editorial Board ensures that significant developments in engineering from around the world are reflected in the Journal. Some important topics covers by journal are nuclear engineering, mechanical engineering, computer engineering, electrical engineering, civil & structural engineering etc.

The coverage of the journal includes all new theoretical and experimental findings in the fields of engineering which enhance the knowledge of scientist, industrials, researchers and all those persons who are coupled with engineering field. IJE objective is to publish articles that are not only technically proficient but also contains information and ideas of fresh interest for International readership. IJE aims to handle submissions courteously and promptly. IJE objectives are to promote and extend the use of all methods in the principal disciplines of Engineering.

IJE editors understand that how much it is important for authors and researchers to have their work published with a minimum delay after submission of their papers. They also strongly believe that the direct communication between the editors and authors are important for the welfare, quality and wellbeing of the Journal and its readers. Therefore, all activities from paper submission to paper publication are controlled through electronic systems that include electronic submission, editorial panel and review system that ensures rapid decision with least delays in the publication processes.

To build its international reputation, we are disseminating the publication information through Google Books, Google Scholar, Directory of Open Access Journals (DOAJ), Open J Gate, ScientificCommons, Docstoc and many more. Our International Editors are working on establishing ISI listing and a good impact factor for IJE. We would like to remind you that the success of our journal depends directly on the number of quality articles submitted for review. Accordingly, we would like to request your participation by submitting quality manuscripts for review and encouraging your colleagues to submit quality manuscripts for review. One of the great benefits we can provide to our prospective authors is the mentoring nature of our review

process. IJE provides authors with high quality, helpful reviews that are shaped to assist authors in improving their manuscripts.

Editorial Board Members

International Journal of Engineering (IJE)

Editorial Board

Editor-in-Chief (EiC)

Dr. Kouroush Jenab
Ryerson University (Canada)

Associate Editors (AEiCs)

Professor. Ernest Baafi
University of Wollongong (Australia)

Dr. Tarek M. Sobh
University of Bridgeport (United States of America)

Professor. Ziad Saghir
Ryerson University (Canada)

Professor. Ridha Gharbi
Kuwait University (Kuwait)

Professor. Mojtaba Azhari
Isfahan University of Technology (Iran)

Dr. Cheng-Xian (Charlie) Lin
University of Tennessee (United States of America)

Editorial Board Members (EBMs)

Dr. Dhanapal Durai Dominic P
Universiti Teknologi Petronas (Malaysia)

Professor. Jing Zhang
University of Alaska Fairbanks (United States of America)

Dr. Tao Chen
Nanyang Technological University (Singapore)

Dr. Oscar Hui
University of Hong Kong (Hong Kong)

Professor. Sasikumaran Sreedharan
King Khalid University (Saudi Arabia)

Assistant Professor. Javad Nematian
University of Tabriz (Iran)

Dr. Bonny Banerjee
Senior Scientist at Audigence *(United States of America)*

Associate Professor. Khalifa Saif Al-Jabri
Sultan Qaboos University (Oman)

Table of Content

Volume 4, Issue 3, July 2010.

Pages

- 201 - 209 Multiband Cross Dipole Antenna Based On the Triangular and Quadratic Fractal Koch Curve
Fawwaz Jinan Jibrael
- 210- 218 Analogy between Student Perception of Educational Space Dimensions and Size Perspective in 3D Virtual Worlds versus Physical World
Noha Saleeb, Georgios Dafoulas
- 219- 232 High Gain Multiband Loaded Inverted-F Antennas for Mobile WiMAX, Wi-Fi, Bluetooth, and WLAN Operation
Debabrata Kumar Karmokar, Khaled Mahbub Morshed, Abu Md. Numan-Al-Mobin, A. N. M. Enamul Kabir
- 233 - 242 Solution algorithms for a deterministic replacement problem
Zakir H. Ahmed
- 243 - 253 Optimal Sensing for Opportunistic Spectrum Access in Cognitive Radio
Nasrullah Armi, Naufal M. Saad, M. Zuki Yusoff, Muhammad Arshad

254 - 261 Pre-Filtering In Robust Model Estimation-A Brief Tour
Dalvinder kaur, Lillie Dewan

Multiband Cross Dipole Antenna Based On the Triangular and Quadratic Fractal Koch Curve

Fawwaz Jinan Jibrael

fawaz_eng2007@yahoo.com

*Department of Electrical and Electronic Engineering
Communication Division
University of Technology
P.O. Box 35010, Baghdad, Iraq*

Abstract

This paper present the analysis and design a small size, low profile and multiband fractal cross dipole antenna. The proposed antenna design, analysis and characterization had been performed using the method of moments (MoM) technique. The new designed antenna has operating frequencies of 0.543 GHz, 2 GHz, and 6.5 GHz with acceptable bandwidth which has useful applications in communication systems. The radiation characteristics and reflection coefficient of the proposed antenna were described and simulated using 4NEC2 software package. Also, the gain of this proposed antenna is calculated and described in the three planes are XZ-plane, YZ-plane, and XY-plane, where the antenna placed in the free space.

Keywords: cross dipole antenna, Koch curve, multiband antenna

1. INTRODUCTION

In modern wireless communication systems and in other increasing wireless applications, wider bandwidth, multiband and low profile antennas are in great demand for both commercial and military applications. This has initiated antenna research in various directions. The telecom operators and equipment manufacturers can produce variety of communications systems, like cellular communications, global positioning, satellite communications, and others. Each one of these systems operates at several frequency bands. To serve the users, each system needs to have an antenna that has to work in the frequency band employed for the specific system. The tendency during last year's had been used one antenna for each system, but this solution is inefficient in terms of space usage, and it is very expensive [1].

The term fractal means broken (fragmented), was coined less than twenty-five years ago by one of history's most creative mathematicians, Benoit Mandelbrot, whose seminal work, "The Fractal Geometry of Nature" [2]. He shows that many fractals exist in nature and that fractals could accurately model certain irregularly shaped objects or spatially non uniform phenomena in nature that cannot be accommodated by Euclidean geometry, such as trees or mountains, this means that fractals operate in non-integer dimension. By furthering the idea of a fractional dimension, he coined the term fractal. Mandelbrot defined fractal as a fragmented geometric shape that can be subdivided in parts, each of which is (at least approximately) a reduced-size copy of the whole. In the mathematics, fractals are a class of complex geometric shapes commonly exhibit the property of self similarity, such that small portion of it can be viewed as a reduced scale replica of the whole. Fractals can be either random or deterministic [3]. Since the pioneering work of Mandelbrot and others, a wide variety of applications for fractals has been found in many branches of science and engineering. One such area is fractal electrodynamics [4-8], in which fractal geometry is combined with electromagnetic theory for the purpose of investigating a new class of radiation, propagation, and scattering problems. One of the most promising areas of fractal electrodynamics research is in its application to antenna theory and design. Fractal antennas have improved impedance and voltage standing wave ratio (VSWR) performance on a reduced physical area when compared to non fractal Euclidean geometries.

In many cases, the use of fractal element antennas can simplify circuit design. Another beneficial of fractal antennas is that, fractal antennas are in form of a printed on the circuit board (PCB) [9].

2. GENERATION OF TRIANGULAR AND QUADRATIC KOCH CURVE GEOMETRIES

Generation of Triangular Koch Curve

The method of construction of the Koch curve is illustrated in (Figure 1). The Koch curve is simply constructed using an iterative procedure beginning with the initiator of the set as the unit line segment (step $n = 0$ in the figure). The unit line segment is divided into thirds, and the middle third is removed. The middle third is then replaced with two equal segments, both one-third in length, which form an equilateral triangle (step $n = 1$); this step is the generator of the curve. At the next step ($n = 2$), the middle third is removed from each of the four segments and each is replaced with two equal segments as before. This process is repeated to infinite number of times to produce the Koch curve. A noticeable property of the Koch curve is that it is seemingly infinite in length. This may be seen from the construction process. At each step n , in its generation, the length of the pre-fractal curve increases to $4/3L_{n-1}$, where L_{n-1} is the length of the curve in the preceding step [10].

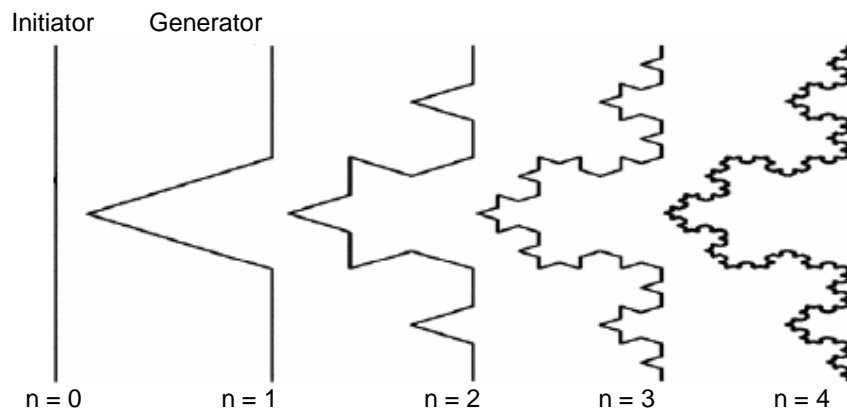


FIGURE 1: The first four iterations in the construction of the triangular Koch curve

Fractal dimension contains used information about the self-similarity and the space-filling properties of any fractal structures [10]. The fractal similarity dimension (FD) is defined as [11]:

$$FD = \frac{\log(N)}{\log(1/\varepsilon)} = \frac{\log(4)}{\log(3)} = 1.26186$$

Where N is the total number of distinct copies, and $(1/\varepsilon)$ is the reduction factor value which means how will be the length of the new side with respect to the original side length.

Generation of Quadratic Koch Curve

(Figure 2) Contains the first three iterations in the construction of the quadratic Koch curve. This curve is generated by repeatedly replacing each line segment, composed of four quarters, with the generator consisting of eight pieces, each one quarter long (see Figure 2) [11]. Each smaller segment of the curve is an exact replica of the whole curve. There are eight such segments making up the curve, each one represents a one-quarter reduction of the original curve. Different from Euclidean geometries, fractal geometries are characterized by their non-integer dimensions. Fractal dimension contains used information about the self-

similarity and the space-filling properties of any fractal structures [10]. The fractal similarity dimension (FD) is defined as [11]:

$$FD = \frac{\log(N)}{\log(1/\varepsilon)} = \frac{\log(8)}{\log(4)} = 1.5$$

Where N is the total number of distinct copies, and $(1/\varepsilon)$ is the reduction factor value which means how will be the length of the new side with respect to the original side length.

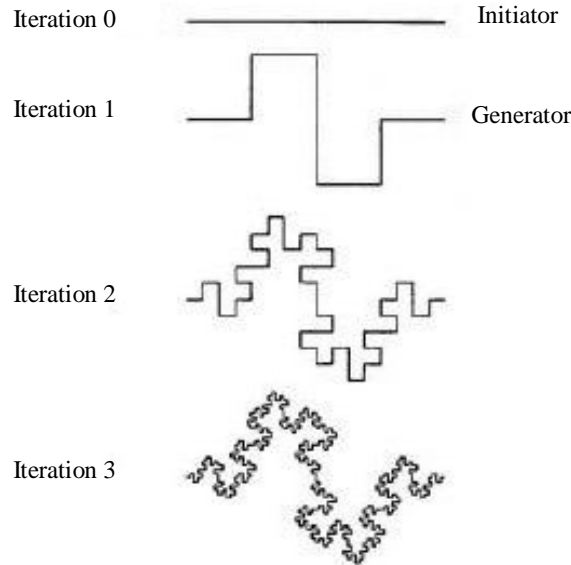


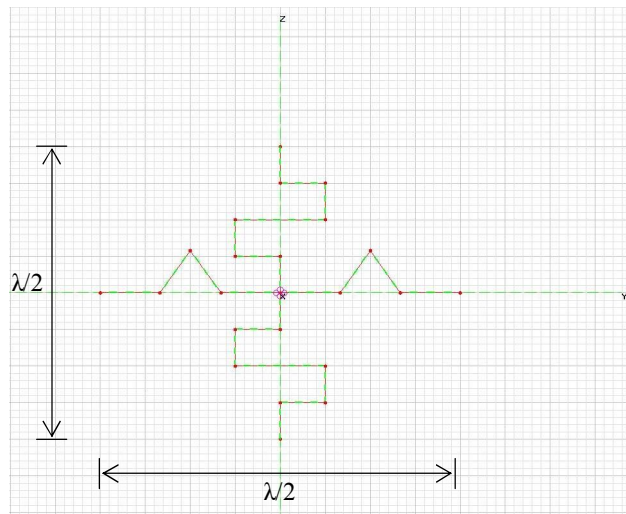
FIGURE 2: First three iterations of the construction of the quadratic Koch curve

3. PROPOSED ANTENNA DESIGN AND SIMULATION RESULTS

In this work, method of moment simulation code (NEC) is used to perform a detailed study of VSWR, reflection coefficient, and radiation pattern characteristics of the cross Koch dipole antenna in free space. The NEC is a computer code based on the method of moment for analyzing the electromagnetic response of an arbitrary structure consisting of wires or surfaces, such as Hilbert and Koch curves. The Method of Moment (MoM) is used to calculate the current distribution along the cross fractal Koch curve antenna, and hence the radiation characteristics of the antenna [12]. The modeling process is simply done by dividing all straight wires into short segments where the current in one segment is considered constant along the length of the short segment [13]. The proposed antenna includes the replacement of each arm in the normal dipole crossed antenna in (Figure 3a) with first-iteration Koch curve geometry. The vertical arm in the normal dipole crossed antenna is replaced with quadratic Koch curve geometry while the horizontal arm in the normal dipole crossed antenna is replaced with triangular Koch curve geometry. The proposed antenna is shown in (Figure 3b). The proposed antenna is placed in YZ-plane with design frequency equal to 750 MHz. The feed source point of this antenna is placed at the origin (0,0,0), and this source is set to 1 volt. For the design frequency of 750 MHz, the design wavelength, λ_0 is 0.4 m (40 cm) then the length of the corresponding $\lambda/2$ dipole antenna length will be of 20 cm. (Figure 4) shows the visualization of this cross dipole antenna geometry by using NEC-viewer software.



(a)



(b)

FIGURE 3: Cross Dipole Antenna (a) cross normal dipole antenna (b) proposed cross dipole antenna

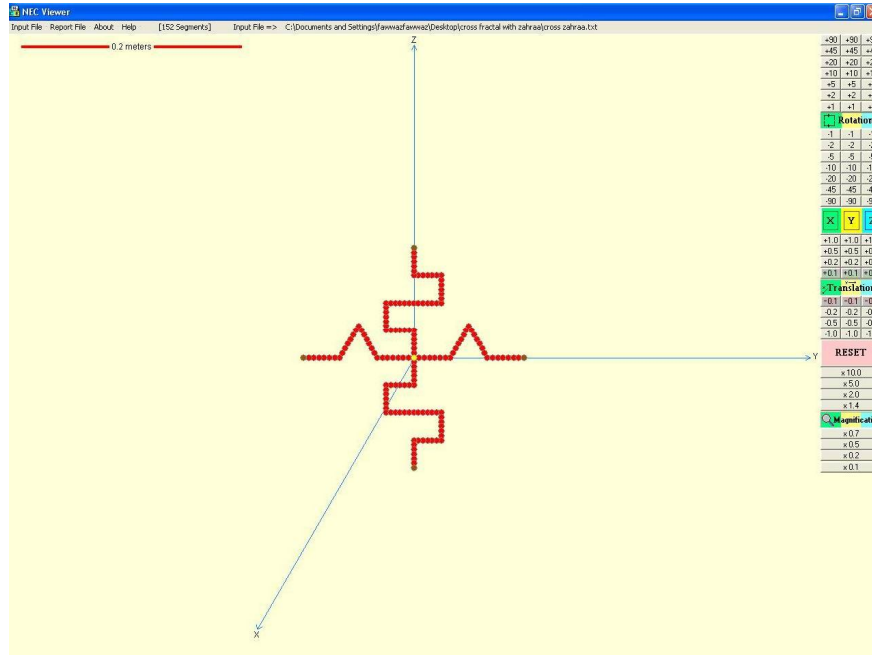


FIGURE 4: Visualization of the modeled cross fractal dipole antenna geometry

The reflection coefficient of the proposed antenna is shown in (Figure 5). it is found that the antenna has triple bands behavior at the resonance frequencies 0.543 GHz, 2 GHz, and 6.5 GHz with reflection coefficient < -10 dB.

(Table 1) shows these resonant frequencies and VSWR and reflection coefficients for each frequency, while (Table 2) shows the gain of each frequency in the three planes XZ-plane, YZ-plane, and XY-plane, where the antenna is placed in the YZ-plane.

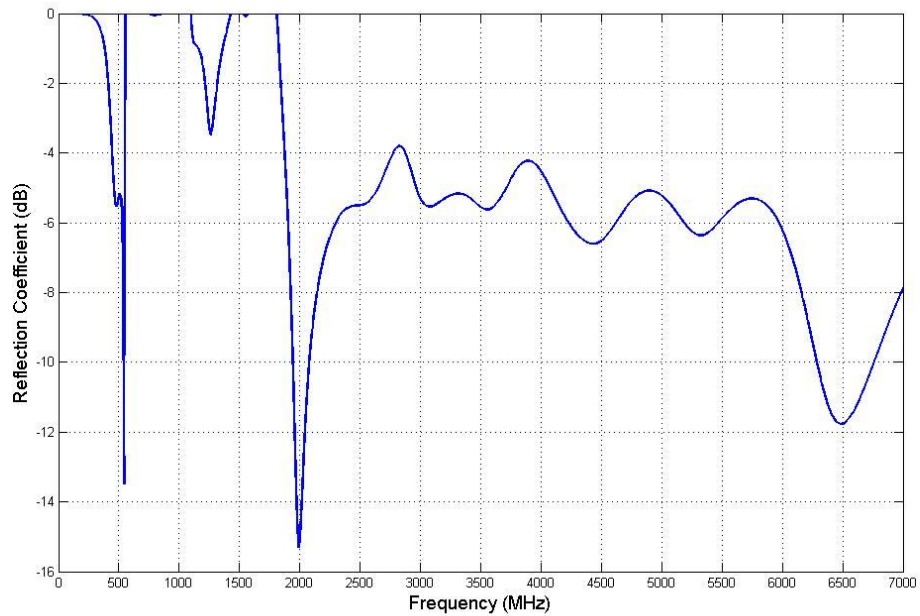


FIGURE 5: Reflection coefficients at the antenna terminals

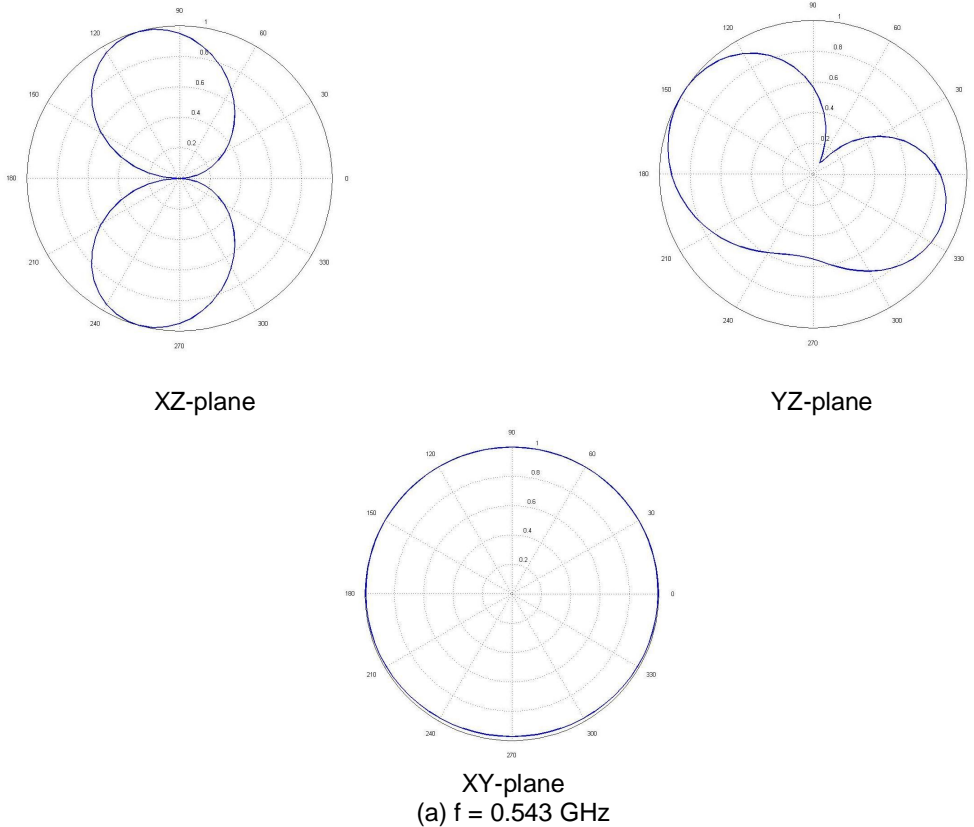
Frequency (GHz)	VSWR	Reflection coefficient (dB)	Bandwidth (GHz)
0.543	1.537	-13.487	0.009
2	1.4231	-15.159	0.14
6.5	1.696	-11.766	0.472

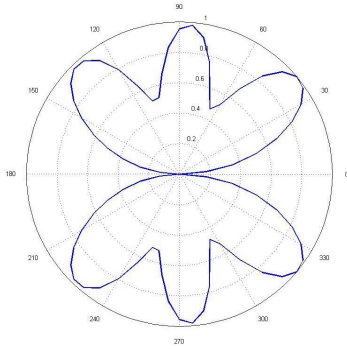
TABLE 1: VSWR and reflection coefficient of the Proposed Antenna

Frequency (GHz)	Gain (dBi)		
	XZ-plane (phi=0)	YZ-plane (phi=90)	XY-plane (theta=90)
0.543	2.04	1.6	1.78
2	1.85	4.42	5.1
6.5	3.57	1.74	4.75

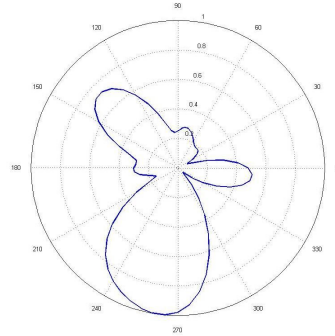
TABLE 2: The Gain of the Proposed Antenna at the Resonant Frequencies in the Three Planes

The radiation patterns at these resonant frequencies in the planes YZ-plane, XZ-plane, and XY-plane are depicted in (Figure 6), where the antenna is placed in the YZ-plane.

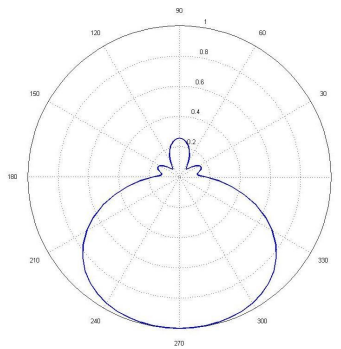




XZ-plane

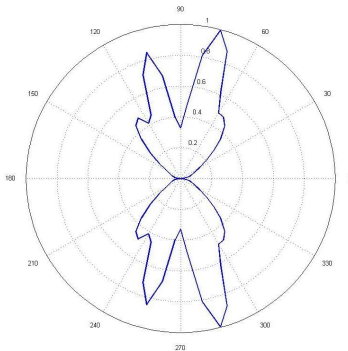


YZ-plane

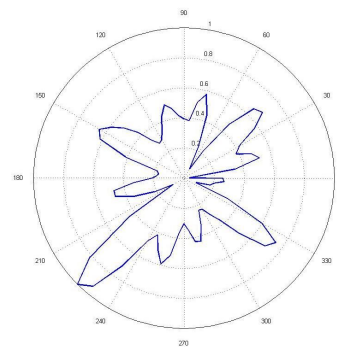


XY-plane

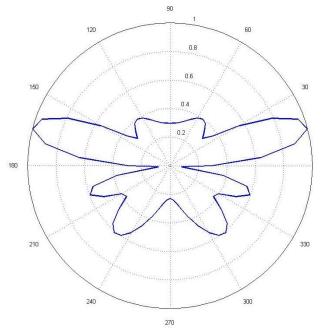
(b) $f = 2$ GHz



XZ-plane



YZ-plane



XY-plane

(c) $f = 6.5$ GHz

Figure 6 Radiation Patterns of the Modeled Antenna at Resonant Frequencies of (a) $f = 0.543$ GHz, (b) $f = 2$ GHz, (c) $f = 6.5$ GHz.

4. CONCLUSION

A novel small size multi-band cross dipole antenna based on a fractal first iteration quadratic and triangular Koch curve, has is presented. The analysis of the proposed antenna is performed using the method of moments (MOM), and the numerical simulations show that the proposed antenna has the ability to work as multi-band antenna at the frequencies 0.543 GHz, 2 GHz, and 6.5 GHz with acceptable bandwidth. In addition, this antenna has VSWR < 2 (reflection coefficient < -10 dB) at all aforementioned resonance frequencies with high gain. The compact size of the antenna geometry makes it useful for wireless applications.

5. REFERENCES

1. J. S. Hong and M. J. Lancaster, "Microstrip Filters for RF/Microwave Applications", New York: Wiley, 2001.
2. B. B. Mandelbrot, "The Fractal Geometry of Nature," W.H. Freeman and company, New York, 1983.
3. X. Yang, J. Chiochetti, D. Papadopoulos and L. Susman. "Fractal Antenna Elements and Arrays". Applied Microwave and Wireless, vol. 5, no. 11, pp. 34-46, May 1999.
4. D. L. Jaggard, "On Fractal Electrodynamics", in H. N. Kritikos and D. L. Jaggard (eds.), Recent Advances in Electromagnetic theory, New York, Springer-Verlag, 1990, pp. 183-224.
5. D. L. Jaggard, "Fractal Electrodynamics and Modelling", in H. L. Bertoni and L. B. Felson (eds.), Directions in Electromagnetic Wave Modelling, New York, Plenum Publishing Co., 1991, pp. 435-446.
6. D. L. Jaggard, "Fractal Electrodynamics: Wave Interactions with Discretely Self-Similar Structures", in C. Baum and H. Kritikos (eds.), Electromagnetic Symmetry, Washington DC, Taylor and Francis Publishers, 1995, pp. 231-281.
7. D. H. Werner, "An Overview of Fractal Electrodynamics Research", in Proceedings of the 11th Annual Review of Progress in Applied Computational Electromagnetics (ACES), Volume II, (Naval Postgraduate School, Monterey, CA, March, 1995), pp. 964-969.
8. D. L. Jaggard, "Fractal Electrodynamics: From Super Antennas to Superlattices", in J. L. Vehel, E. Lutton, and C. Tricot (eds.), Fractals in Engineering, New York, Springer-Verlag, 1997, pp. 204-221.
9. D. Kalra, "Antenna Miniaturization Using Fractals," M.Sc. Thesis, University of Deemed, India, 2007.

- 10.K. Falconer, "*Fractal Geometry; Mathematical Foundations and Applications*," 2nd Edition, John Wiley and Sons Ltd., 2003.
- 11.Paul S. Addison, "*Fractals and Chaos*", Institute of Physics Publishing. The Institute of Physics, London, 1997.
- 12.C. A. Balanis, "*Antenna Theory: Analysis and Design*", 3rd ed., Wiley, 2005.
- 13.G. J. Burke and A. J. Poggio, "Numerical Electromagnetic Code (NEC)-Program description," January, 1981, Lawrence Livermore Laboratory.

Analogy between Student Perception of Educational Space Dimensions and Size Perspective in 3D Virtual Worlds versus Physical World

Noha Saleeb

*School of Engineering and Information Sciences
Middlesex University
London, UK*

N.Saleeb@mdx.ac.uk

Georgios Dafoulas

*School of Engineering and Information Sciences
Middlesex University
London, UK*

G.Dafoulas@mdx.ac.uk

Abstract

One of the prominent practices currently associated with 3D virtual worlds, such as Second Life, is their increased utilization as 3D virtual learning environments (3D VLEs). This study is part of a research in progress dedicated to evaluate different engineering design aspects of these emergent VLEs, and define the impact of their design features on delivering online education. The aim of this paper is to investigate and analogize between users' perception of space in virtual worlds compared to its corresponding perception in the physical world in terms of area size, dimensions and overall 3D visual perspective. This is achieved by recording the visual estimations of different student categories, within diverse 3D virtual sites, in response to survey questions depicting space size and capacity for holding students and hosting e-learning sessions. Furthermore, the differences in student responses are analyzed and elucidated in order to formulate a hypothesis about how similar or dissimilar users perceive spaces in 3D virtual worlds in comparison with the physical world.

Keywords: visual perception in 3D virtual worlds, virtual learning environments, educational facilities in Second Life, class capacity in e-learning spaces.

1. INTRODUCTION

Since the onset of 3D virtual worlds, whether used for gaming purposes or as learning environments, 3D designers and builders have strived to create virtual constructions within them that have proved to be both innovative and imaginative but also comfortably familiar for the user [1]. This flourishing in 3D virtual design has been the result of the vast disparity between the physical world and virtual worlds in terms of diminished constraints to free design [2], for as previously asserted by Bourdakos and Charitos [3], the nature of space in virtual environments (VEs) is fundamentally different from the nature of real space and thus subsequently the architecture of VEs requires new theory and practice. Examples of these fundamental differences include the non-presence of gravity, material and budget restraints, which have given rise to many known and novel building styles in VEs such as Photo-realistic (identical replica of existing

in reality), artistically-realistic (similar to existing in reality), functionally-realistic (has no equivalent in reality but is realistically designed), metaphorically-realistic (entails realistic functions), hybrid (mixture of realistic and imaginative design), fantasy (imaginative design defying reality), and abstract (ambiguous design) [4].

In 3D virtual places, designers are increasingly faced with higher-degree spatial organization than in the physical world, comprising the cognitive relationship between content and space [1]. Cognition is a process proclaimed on the user's sensory-motor and neurological systems. The process of visual acquiring, assimilation and interpretation of environmental information is called cognitive mapping to understand the relationship between the objects in a space [5]. Therefore, since Downs and Stea [6] denote that "human spatial behavior is dependent on the individual's cognitive map of the spatial environment", this indicates that a user's perception of the virtual space within a 3D VE can control his conduct within this virtual environment. This would accordingly also imply that students' perception of their learning spaces in 3D VEs would hence affect their behavior inside them. It is thus the focus of this paper to investigate how students' perception of 3D virtual e-learning spaces differs from their perception of physical learning spaces in an attempt to explore whether this affects their overall learning process. Results of this research can subsequently help educators and designers in VEs to enhance the architectural design of virtual 3D learning spaces in VEs to be more suitable for students' e-learning within them.

2. BACKGROUND

The effect of physical spaces on students' learning in general has been amply asserted in previous literature. Oladipupo and Oyelade [7] state that "there is more to students' failure than the students' ability". According to Kenchakkanavar and Joshi [8], incompatibility of classrooms for teaching was one of the factors affecting student failures in their courses. Furthermore it has been demonstrated that classes smaller than 900 sq. ft. in area are undesirable as they do not allow for adequate movement between tables without bumping into students and their belongings; crowded classrooms contribute to discipline problems [9]. However if a 900 sq. ft. class is built inside a VE, will the students perceive it as the same size as in the physical world, or smaller or larger, and thus will it be adequate for their needs? Moreover, narrow hallways that are too small for student traffic between classes have been found to encourage fighting and hinder evacuation in emergencies [10]. Again here while corridors of 2m width might be acceptable in the physical world, would this width be perceived as sufficient in the virtual world? It is therefore imperative in the case of 3D virtual learning environments to inquire into how a student identifies with the surrounding spaces, perceives dimensions, shape, and perspective and how that is different from perceiving the totality of spaces in the physical world. This realization is essential since if differences prevail between the virtual and physical worlds in perception of space size, then this necessitates a change in the engineering codes and guidelines used by educators, designers, builders and architects to build inside 3D VEs to counteract for these differences in perception.

Hence, in agreement with Lau and Maher [1], orienting users within efficiently designed spaces in a virtual environment requires a "detailed study of environmental cognition". Cognition and visualization involve graphic rendering of data in such a way to take advantage of the human ability to recognize patterns and see structures [11]. To understand how these cognitive principles can be applied to the design of VEs, experiments with users, namely students in this study, are required to capture students' different perceptions of the 3D spaces they experience during their e-learning sessions. To pursue this notion, it is necessary to initially differentiate between the different types of user viewpoints available within 3D VEs. While participants have the capability to observe the environment from many perspectives [12], there are two basic types of perspective viewpoints in 3D VEs: i) virtual reality perspective and ii) virtual world perspective [13]:

Virtual reality can be defined as an environment created by the computer in which the user feels immersed perceptually and psychologically in the digital environment [14]. The main difference between virtual reality and virtual world viewpoint is the way the user experiences the virtual

environment. If the VE is experienced through the first person i.e. seeing the world through the eyes of the avatar and surrounded by the environment, then this is virtual reality [15]. This perspective or viewpoint can be achieved by manipulating camera controls in the VE (or wearing head mounted display devices) and is the closest to “real life” physical perspective. In contrast, virtual world view allows the user to see the VE in 3rd person by watching the avatar move at a distance inside the VE [13]. These differences result in different spatial cognition by the users [16].

The focus of this paper is to investigate the difference in student perception for 3D virtual space size and dimensions, versus the “real-life” physical perception, using the “virtual world” (3rd person) perspective explained beforehand.

3. RESEARCH RATIONALE AND METHODS

The “virtual world” perspective tested in this study is the default viewpoint utilized within 3D VLEs in general and the more commonly used among students for navigation in 3D VLEs. In order to capture the difference between students’ perception of space size between the virtual world and the physical world, the subsequent research rationale and techniques were followed:

Several randomized samples of students from different categories (elaborated henceforth) were asked to participate in short consecutive e-learning sessions inside 15 selected 3D virtual learning spaces, inside which students were encouraged to navigate, using the “virtual world” viewpoint, to assimilate the extent of the space size by being immersed inside each (explained henceforth). At the end of the time spent inside each virtual site, the students were all asked to record how many users they perceived this space could hold by choosing from a list of predetermined ranges, also described consequently. Other closed ended questions were asked of the students related to assessing more engineering and architectural design elements of the space, but which are not the focus of this paper at hand. The numerical results offered by the students concerning their perceptions were then averaged for each 3D virtual site used, and these results were compared to the actual number of students that each site would actually hold if built in the physical world with the exact same dimensions. This comparison was used to identify whether space in virtual digitized worlds is recognized by users as being the same size as that in reality or larger or smaller.

The study was conducted in Second Life as a representative of 3D Virtual Learning Environments for its popularity among universities and educational institutions for delivering e-learning [17]. The samples of consenting participants in this study were 84 students from the School of Engineering and Information Sciences at Middlesex University. They were divided into 31 under graduate students, 33 post graduate students, and 20 members of staff representing adult learners. The participants were diverse in gender and cultural background. Results taken from all 3 categories of students were analyzed comparatively and relevant conclusions were drawn accordingly.

The 15 selected 3D virtual learning spaces were chosen to represent a diverse number of variations in space design characteristics in terms of:

- space shape (e.g. circular, rectangle, square)
- size (e.g. small, medium, large – criteria for size naming explained hereafter)
- dimension ratio (width:length:height e.g. 2:2:1)
- openness of space (i.e. whether space is confined by walls or not)

This variety in choice was essential in order to identify if there were any prominent architectural design factors affecting student perception of spaces in 3D VLEs.

The ranges of answers that the students were asked to answer from included:

- space can withstand: 10 - 30 students
- space can withstand: 40 - 60 students
- space can withstand: 70 - 100 students or more

The above three answering criteria were determined based on real-life physical classroom classifications where i) classrooms are considered “small” size learning spaces with capacity up to 28 students. If $2.5 - 3\text{m}^2$ is required per student, then the average area of a classroom would be $25-75\text{m}^2$. Educational spaces with similar area size in Second life were used as examples of small learning spaces. ii) Seminar rooms are considered “medium” size learning spaces with capacity of 45-60 students. If $2.2-2.6\text{m}^2$ is required per student in a seminar room, then the average area would be $100-150\text{m}^2$. Educational spaces with similar area size in Second life were used as examples of medium learning spaces. iii) Lecture auditoriums are considered “large” size learning spaces with capacity of up to 200 students. If $1.6-2\text{m}^2$ is required per student in a lecture hall, then the average area would be greater than 150m^2 . Educational spaces with similar area size in Second life were used as examples of large learning spaces [18] [19]. Learning spaces holding over 100 students were rare in Second Life since the current servers’ capabilities cannot withstand more than this number of logged in users at the same time on the same site. Each learning space used within this study was also classified as “open” if it did not contain surrounding walls.

The equation used to calculate the average perceived number of users by students from each category for each site was:

$$\left(\begin{array}{l} (\text{no. of “10-30” votes} * 30) + \\ (\text{no. of “40-60” votes} * 60) + \\ (\text{no. of “70-100” votes} * 100) \end{array} \right) / \text{Total number of participants}$$

As an additional analysis, the standard deviation between the results of under graduate students, post graduate students and adult learners was also calculated to find the discrepancy between the values and how this may be related to different types of educational space shapes, sizes and dimensions. The standard deviation measures the spread of the data around the mean value and thus how widely dispersed they are from the maximum to the minimum value. The larger the value of the standard deviation the more this implies that the individual data points are farther from the average value. To calculate the standard deviation, the mean value is first calculated. Next, the deviation of each data point from the average is calculated by subtracting its value from the mean value. Each deviation is squared, and the individual squared deviations are averaged together. The resulting value is known as the variance. Standard deviation is the square root of the variance [20].

Diagrams illustrating the different findings were created accordingly, as demonstrated in the subsequent sections.

4. RESULTS

Results in this paper were identified in three areas in accordance with the aims and focus of this study:

- A comparison between the results obtained from under graduate, post graduate and adult learners concerning their perception of the number of users that each 3D virtual learning space in consideration can withstand.
- An analogy to compare between the overall students’ average perceived number of users for each site (and thus what area size is implied for that site) versus the actual number of users that could be withheld if this learning space was built with the exact same dimensions in the physical world.
- Calculate the standard deviation between the results of the three student categories, for each 3D virtual site, to find out factors affecting different perceptions by students.

4.1 Capacity of Users Perceived for each 3D Virtual Learning Space

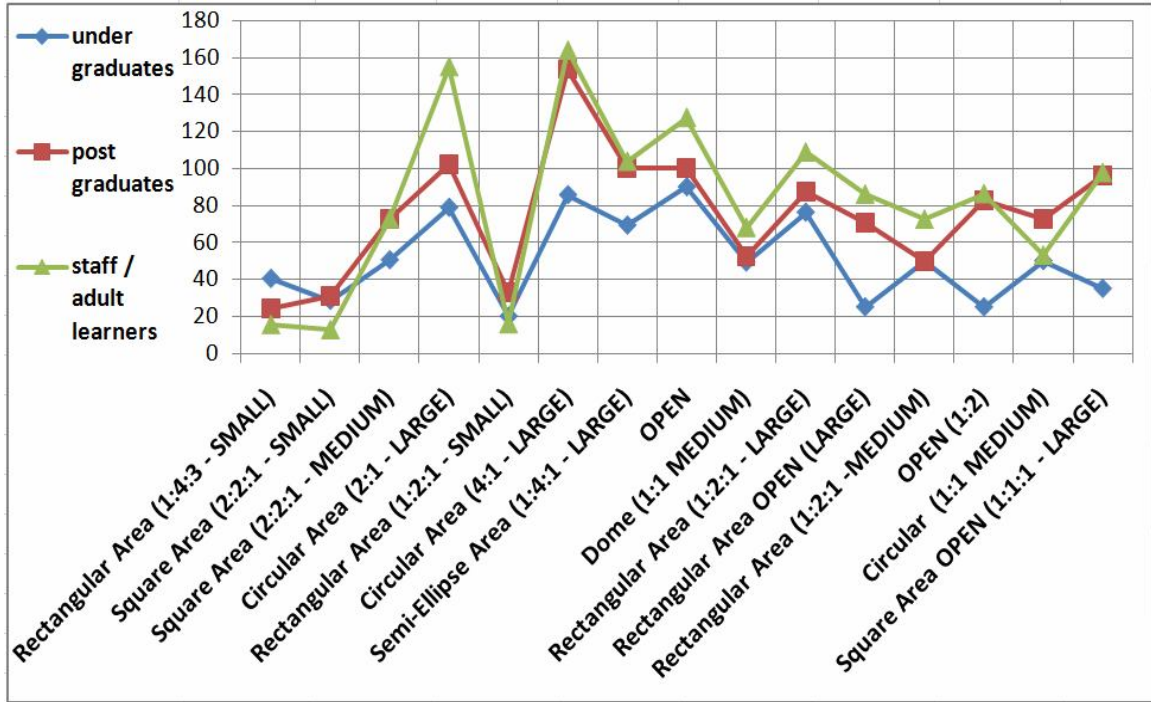


FIGURE 1: Average number of users that can be withheld in each site as perceived by different categories of students

The former Figure 1 illustrates the perceived number of users that each category of students (under graduate, post graduate and adult learners) estimated can be withheld inside each of the 15 3D virtual learning spaces selected for this study.

As evident from the figure, it can be clearly noticed that average number of users perceived by under graduate students for the different sites in general tends to be lower than results depicted by the other two categories of students for all sites. Even more, while demonstrated results for post graduate students are higher than those for under graduate students, they are still lower than those offered by adult learners, who give the highest capacity of students for all sites. This can provide a general trend where the older the age category, the larger the students' perception is of the size of the 3D virtual learning space and the capacity of users it can hold. The implications of these findings are to be discussed in the conclusions.

4.2 Average Perceived Number of Users and Size of each Site compared to the Actual Space Size

The average perceived numbers of users for each site demonstrated in Figure 2 denote the mean values for all three combined categories of students for each 3D virtual site. It can be evidently seen that the students' overall estimation for the number of users withheld in each site (and thus also approximation for the size of the space) is very similar to the actual number and size ranges of each space. Small, medium and large spaces were correctly identified by students by correctly estimating the number of users that should be within each space. This result holds true despite the differences in the learning space shape, dimensions ratio, and openness of walls differentiating the architectural design of the 3D virtual spaces from each other. The implications of this result are to be discussed consequently.

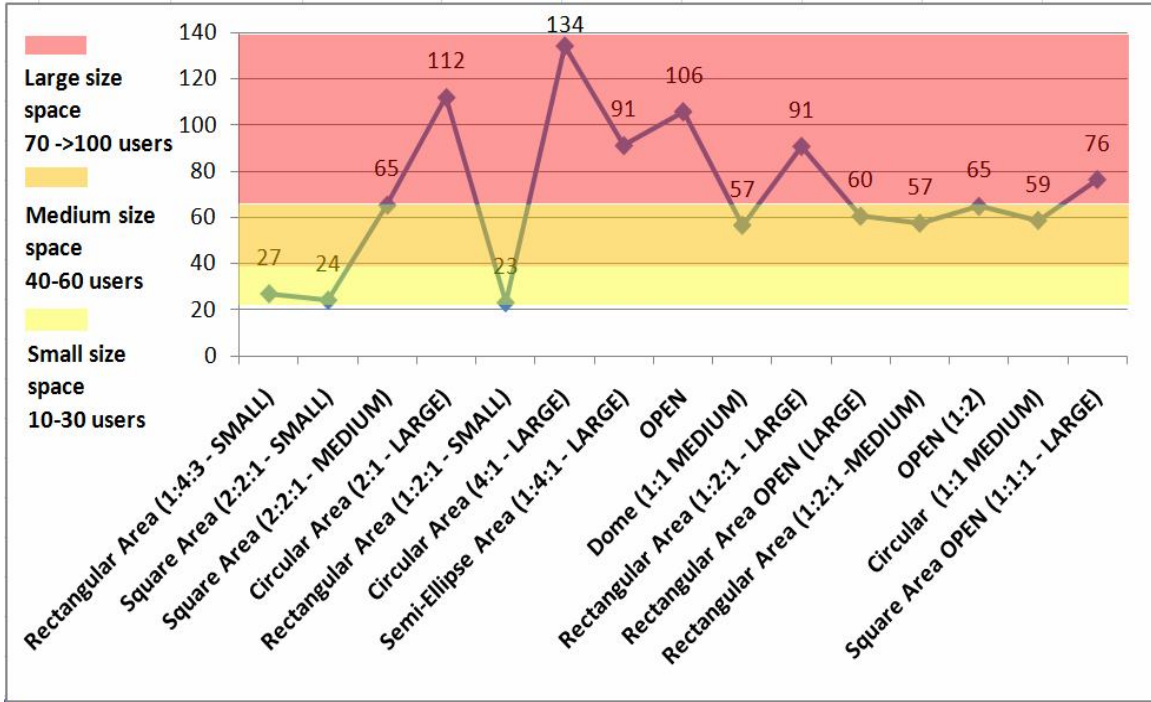


FIGURE 2: Correspondence of number of perceived students per site to the actual capacity and size of each site

4.3 Standard Deviation between the Response Ranges of the Student Categories

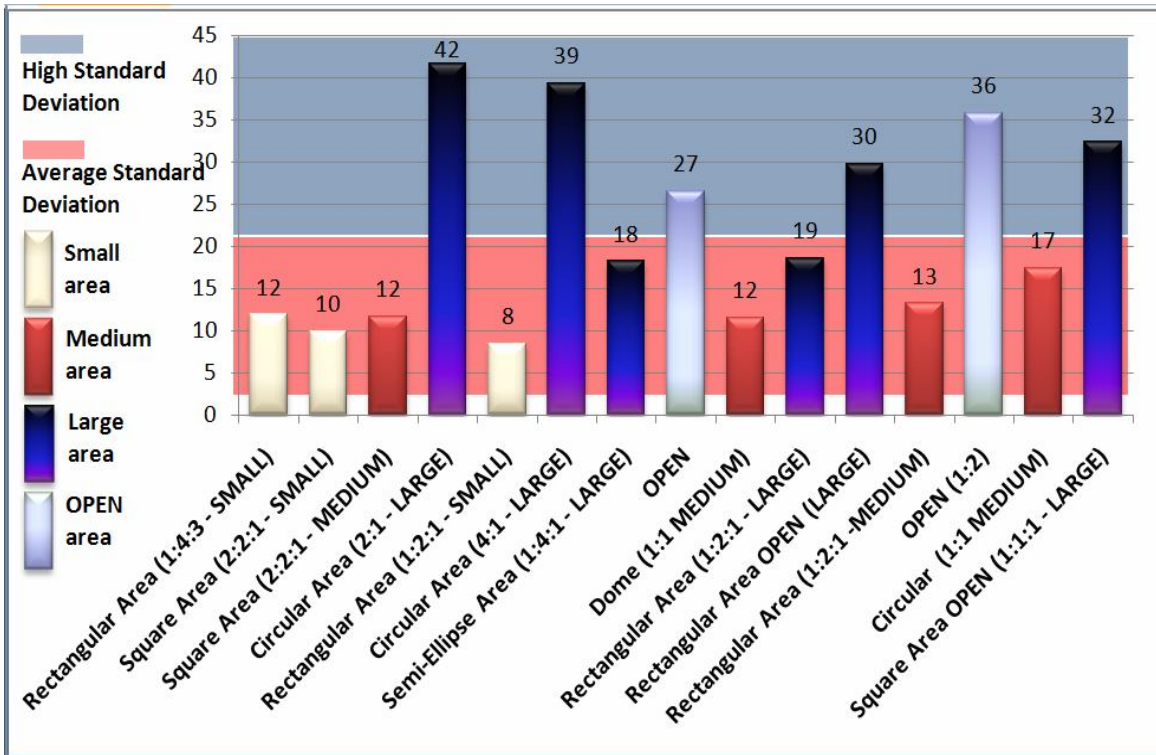


FIGURE 3: Standard deviation calculated between responses of different student categories for each 3D virtual site

Figure 3 displays the calculated standard deviation between the highest and lowest perceived values of number of users given by the 3 student categories for each site. The purpose of this procedure was to find which virtual spaces offered most uncertainty to students and indecisiveness in estimating the number of users that a space can hold. This is because the greater the difference between the numbers offered by the 3 categories of students for each site, the higher the standard deviation, signifying that there are split opinions regarding the number of users that a space can hold, which means increased uncertainty and inability to visually identify the correct size of the space in concern by all students involved. The sites providing this problem were examined to identify any common architectural design factors between them that might be the cause for this difference between the virtual and physical perception.

The results in Figure 3 clearly show that there was an acceptable and moderate deviation in values (presented by the 3 student categories) for all “small” and “medium” sized 3D virtual learning spaces used in this study (- definition of “small”, “medium” and “large” clarified earlier). However a very high standard deviation could be seen with “large” sized 3D virtual learning spaces which are either circular in area or “open” spaced with no or few encompassing walls. Completely open venues (e.g. outdoors, space etc.) were also very difficult to estimate numbers of users for, producing the same uncertainty. The only types of “large” sized spaces which gave a moderate deviation of results were those containing straight-linear or curved-linear rows of seating. The implications of all the above results are discussed in the following section.

5. CONCLUSION & FUTURE WORK

Three sets of significant results were obtained from this study that will be elaborated on in this section. The whole study was conducted using the “virtual world” perspective for student navigation explained earlier.

It was initially identified that under graduate students have the tendency to under estimate the size of any given 3D virtual learning space compared to post graduates who offer higher numbers and adult learners who offer highest numbers of perceived students for virtual spaces i.e. perceive the space larger than younger groups of students. This can be attributed to the fact that under graduate students are more acquainted with 3D online gaming environments which offer vast terrains and multitudes of buildings thus might cause any individual learning space to seem smaller in comparison to what students are used to in gaming environments. While adult learners provide higher values for perceived numbers of students than post graduate students (i.e. perceive the space size as larger), both results are close which might indicate that more mature students in general estimate space size more realistically and correctly. These results can be useful for educators, designers, architects or builders in general in VLEs by creating design guidelines for building enhanced educational facilities inside 3D Virtual Learning Environments . One design recommendation in this case would be to enlarge the size of the 3D virtual classrooms and learning spaces more than their counterparts in the physical world so as to appear for undergraduates the same size as the physical spaces (after taking into consideration the diminishing visual perception effect experienced by under graduate students in 3D VLEs), or appear for graduates and adult learners as slightly large and thus more comfortable and spacious to learn inside. This added contentment with the space size would help enhance the student e-learning experience in 3D VLEs.

The second set of results attained within this study is related to how accurately students in general estimated the space sizes and perceived them with the same dimensions as they really are. This was done by estimating the correct number of users that can be withheld in each site. The results showed that all virtual spaces were estimated to be within the correct “small”, “medium” or “large” size ranges (with some discrepancy between the 3 different student categories but within the mentioned size ranges e.g. undergraduates perceived them quite smaller as mentioned earlier). Thus, this indicates that visual perception and interpretation of

space size by students in the 3D virtual world in general is very similar to that in the physical world.

The third set of findings, depicting standard deviation between results, shed light on factors which might be attributing to incorrectly understanding and perceiving the 3D virtual space. It was shown that while there were no problems with correctly identifying “small” and “medium” sized spaces, circular shaped “large” size spaces and open spaces caused most confusion and uncertainty for students when attempting to define space size (through identifying number of users inside it). This may be attributed to the fact that absence of boundaries and set seats made it difficult to recognize space sizes correctly and caused this disparity between virtual conception of space and physical conception of space. An additional building recommendation for 3D virtual educational spaces that can be derived from these results can be to assign more defined and distinct seating arrangements for users within circular shaped and open learning spaces to help students perceive the space perspective more accurately.

Future work can be used to provide further evidence for how students perceive the 3D virtual space by creating customized models in Second Life, subjecting students to them and observing their reactions to changing other engineering and architectural design elements in their surroundings. Investigating change of individual dimensions of the space (e.g. height, width, length) on students’ perception of the space and their satisfaction from it can be also subject to future research.

6. REFERENCES

1. K. H. Lau, M. L. Maher, “*Architectural Design and Virtual Worlds*”. Architecture Week, pp.T3.1 (2000)
2. N. Saleeb, G. Dafoulas, “*Architectural Propositions for Enhancement of Learning Spaces within 3D Virtual Learning Environments*”. In Proceedings of the IEEE International Conference on Information Society (i-Society), London, UK (2010).
3. V. Bourdakis, D. Charitos. “*Virtual Environment Design; Defining a new direction for architectural education*”, in Brown, A., Knight, M. & Berridge, P. (eds.), Architectural Computing: From Turing to 2000, Proceedings of the 17th international eCAADe conference, Liverpool, ISBN: 0-9523687-5-7 (1999)
4. S. Minocha, A.J. Reeves. “*Interaction design and usability of learning spaces in 3D multi-user virtual worlds*”, Human Work Interaction Design 2009, Pune, India, (2009)
5. K. Osberg, “*Spatial Cognition in the Virtual Environment*”, from <http://ftp.hitl.washington.edu/projects/education/puzzle/spatial-cognition.html> (1994)
6. R.M. Downs, D. Stea, “*Cognitive Maps and Spatial Behaviour: Process and Products*”, in Image and Environment. Downs, R.M. and Stea, D. (Eds). Edward Arnold. London (1973)
7. O.O. Oladipupo, O.J. Oyelade, “*Knowledge Discovery from Students’ Result Repository: Association Rule Mining Approach*”, International Journal of Computer Science & Security (IJCSS), 4(2), (2010)
8. V.D. Kenchakkanavar, A.K. Joshi, “*Failure Mode and Effect Analysis: A Tool to Enhance Quality in Engineering Education*”, International Journal of Engineering (IJE), 4(1), (2010)
9. J.P. Eberhard, “*A Place to Learn: How Architecture Affects Hearing and Learning*”. The ASHA Leader , 13(14), (2008)

10. L.D. Hall, "*Effect of School Architecture on its students. (Environmental psychology)*". from Design Community Architecture Discussion: <http://www.designcommunity.com/discussion/26903.html> (2001).
11. B. Buxton, "*Snow's two cultures revisited: perspectives on human-computer interface design*". In Linda Jacobson, ed. *CyberArts: exploring art and technology*, pp. 24—38, (1992).
12. M. Bricken, "*Virtual reality learning environments: potentials and challenges*". Human Interface Technology Laboratory Technical Publication No, HITL-P-91-5. Seattle, WA: Human Interface Technology Laboratory, (1991).
13. S. Minocha, "*Design of Learning Spaces in 3-D Virtual Environments*" from <http://www.jisc.ac.uk/media/documents/programmes/elxinstit/ltigdelveppredact.pdf>, (2008).
14. H. McLellan, "*Virtual Realities*". In D. H. Jonassen (Ed.), *Handbook of research for educational communications and technology*, New York: Macmillan, pp. 457-587, (1996).
15. J. Loomis, J. Blascovich and A. Beall, "*Immersive virtual environments as a basic research tool in psychology*". *Behavior Research Methods, Instruments, and Computers*, 31, 557–56, (1999).
16. A. Burton, G. Priestnall, G. Polmear., and N. Mount, "*Real-Time Landscape Visualisation: Experiences in a Teaching and Learning Context.*" Geographical Information Science Research UK (GISRUK) Conference, Manchester Metropolitan University, (2008).
17. B. Joseph, "*Global Kids, Best Practices in using Virtual Worlds for Education*". Second Life Education Workshop, SL Community Convention, Chicago: Word Press, pp. 7-14 (2007).
18. "*Building Space Summary*". Lakewood, Colorado: Jefferson County Educational Specification Space Program, Jefferson County Public Schools, (2007).
19. N. Bayly, B. Brandt, C. Meyers, C. Minihan, D. Raby, "Emory College Classroom Design Guide" from: <http://www.college.emory.edu/about/planning/facilities/classroomGuidelines.pdf> (2008).
20. J. Stanley, "What is standard deviation" from <http://www.wisegeek.com/what-is-standard-deviation.htm> (2010)

High Gain Multiband Loaded Inverted-F Antennas for Mobile WiMAX, Wi-Fi, Bluetooth and WLAN Operation

Debabrata Kumar Karmokar

*Department of Electrical & Electronic Engineering
Khulna University of Engineering & Technology
Khulna-9203, Bangladesh*

debeee_kuet@yahoo.com

Khaled Mahbub Morshed

*Department of Electronics & Communication Engineering
Khulna University of Engineering & Technology
Khulna-9203, Bangladesh*

kmm_ece@yahoo.com

Abu Md. Numan-Al-Mobin

*Department of Electronics & Communication Engineering
Khulna University of Engineering & Technology
Khulna-9203, Bangladesh*

nmobin27@yahoo.com

A. N. M. Enamul Kabir

*Department of Electrical & Electronic Engineering
Khulna University of Engineering & Technology
Khulna-9203, Bangladesh*

anmenamulkabir@eee.kuet.ac.bd

Abstract

Multiband loaded inverted-F antennas (LIFA's) suitable to be applied in a portable device as an internal antenna having high gain property for mobile WiMAX, Wi-Fi, Bluetooth and WLAN operation are presented. The proposed antennas are directly feed by 50 Ω coaxial connector. The antenna arms effectively control the excited resonant modes for the required operation. Total areas occupied by the antennas are 24 x 37 and 29 x 37 mm² in case of slightly loaded IFA (SLIFA) and moderately loaded IFA (MLIFA) respectively. The antennas contain an incredibly high peak gains of 8.31, 8.88 and 6.32 dBi and 8.48, 8.67 and 6.89 dBi for 2.3 GHz mobile WiMAX, 2.4 GHz WLAN/Bluetooth and 5.8 GHz Wi-Fi operation for SLIFA and MLIFA respectively, with less than 0.84 and 1.8 dBi gain variation at lower and upper operating band within the 10 dB return loss bandwidth. In addition, the antennas have achievable bandwidth, return loss and radiation characteristics.

Keywords: Inverted-F antenna, Loaded inverted-F antenna, Worldwide interoperability for microwave access (WiMAX), Wireless-Fidelity (Wi-Fi), Bluetooth, Wireless local area network (WLAN).

1. INTRODUCTION

Bluetooth and WLAN operate in 2.4 GHz industrial, scientific and medical (ISM) band (frequency range 2.4–2.5 GHz) and unlicensed national information infrastructure (U-NII) band used in WLAN, Bluetooth and Wi-Fi operation. This U-NII band can be divided into three sub-bands as

U-NII low (frequency ranges 5.15–5.35 GHz), U-NII mid (frequency range 5.47–5.725 GHz) and U-NII high (frequency range 5.725–5.875 GHz), which offers more non-overlapping channels than the channel offered in the ISM frequency band. On the other hand, IEEE 802.16e-2005 standard named mobile WiMAX provides maximum of 10 Mbps wireless transmission of data using variety of transmission modes from point to multipoint links to portable and fully mobile internet access devices. WiMAX is a possible replacement for cellular technologies such as global system for mobile (GSM) communication, code division multiple access (CDMA) or can be used as an overlay to increase capacity. It has also been considered as a wireless backhaul technology for 2G, 3G and 4G networks in both developed and poor nations. Mobile WiMAX operating bands are 2.3 GHz (frequency range 2.3–2.4 GHz), 2.5 GHz (frequency range 2.5–2.7 GHz) and 3.5 GHz (frequency range 3.4–3.6 GHz). To provide seamless internet access for the mobile devices a dual band antenna for Wi-Fi, mobile WiMAX and WLAN operation is necessary.

The key design configurations in order to meet multiband operation include a monopole antenna feed with SMA connector [1], integrated monopole slot antenna [2], coplanar waveguide (CPW) feed meandered monopole antenna [3], a CPW-fed compact monopole antenna with two resonant paths [4], a CPW-fed tapered bent folded monopole antenna [5], a microstrip-fed double-T monopole antenna [6], a meander-line monopole antenna with a backed microstrip line [7], a C-shaped monopole antenna with a shorted parasitic element [8], and a branched monopole antenna with a truncated ground plane [9], printed monopole antenna for WiMAX/WLAN operation [10]. Microstrip line feed printed antenna [11], printed monopole array [12], T-shaped monopole with shorted L-shaped strip-sleeves [13], microstrip coupled printed planar inverted-F antenna (PIFA) [14], surface mount monopole [15], flat-plate inverted-F antenna (IFA) [16], CPW-fed triangular shaped monopole [17], metal plate [18], internal composite monopole [19], multi slot [20], compact loop [21], compact PIFA [22], flat plate with shorted parasitic element [23], internal PIFA [24], miniaturized PIFA [25], and two strip monopole [26] antenna can support Bluetooth (BT)/WiMAX/Wi-Fi/WLAN operation. Previously, single band antenna for WLAN or Wi-Fi operation, printed quasi-self complementary [27], CPW-fed folded slot monopole [28], CPW-fed shorted F-shaped monopole [29], planar inverted-L antenna [30] and T-shaped monopole [31] have been analyzed and proposed. Inverted-L antenna suffers from lower input impedance than PIFA and slot antennas. In this paper, we present high gain slightly loaded and moderately loaded IFA to support multiband operation.

2. ANTENNA DESIGN

In designing multiband antenna for Wi-Fi, mobile WiMAX and WLAN operation, we examine the possibility of increasing antenna gain with simplified structure. Using method of moments (MoM's) in Numerical Electromagnetic Code (NEC) [32], we conducted parameter studies to ascertain the effect of different loading on the antenna performance to find out the optimal design. For our study we assume the copper conductor and the antenna was intended to be matched to 50 Ω system impedance.

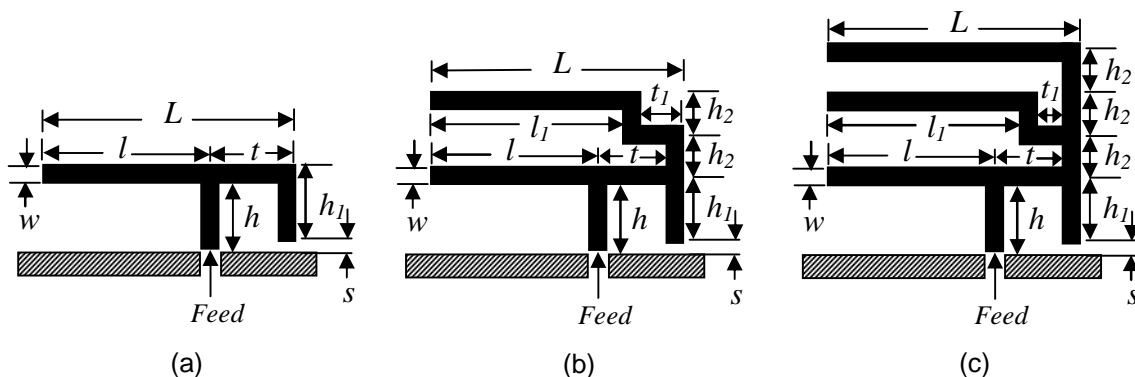


FIGURE 1: Geometry of (a) IFA, (b) SLIFA and (c) MLIFA.

In case of IFA as shown in Figure 1(a), the resonant frequency related to w given as [33]

$$f_1 = \frac{c}{4(l+t+h_1)} \tag{1}$$

Where c is the speed of light. The effective length of the current is $l+t+h_1+w$. Under this case the resonant condition can be expressed as

$$l+t+h_1+w = \frac{\lambda_0}{4} \tag{2}$$

The other resonant frequency that is a part of linear combination with the case $0 < w < (l+t)$ and is expressed as

$$f_2 = \frac{c}{4(l+t+h_1-w)} \tag{3}$$

The resonant frequency (f_r) is a linear combination of resonant frequency associated with the limiting case. For the antenna geometry of Figure 1(a), f_r can be written from equation (1) and (2) as [34]

$$f_r = r.f_1 + (1-r)f_2 \tag{4}$$

Where $r = \frac{w}{l+t}$. With the help of resonant frequency theory of IFA, and impedance matching concept, we consider the dimension of the IFA as $l = 31 \text{ mm}$, $t = 6 \text{ mm}$, $h_1 = 13.6 \text{ mm}$, $h = 14 \text{ mm}$, $s = 0.4 \text{ mm}$, $w = 2 \text{ mm}$.

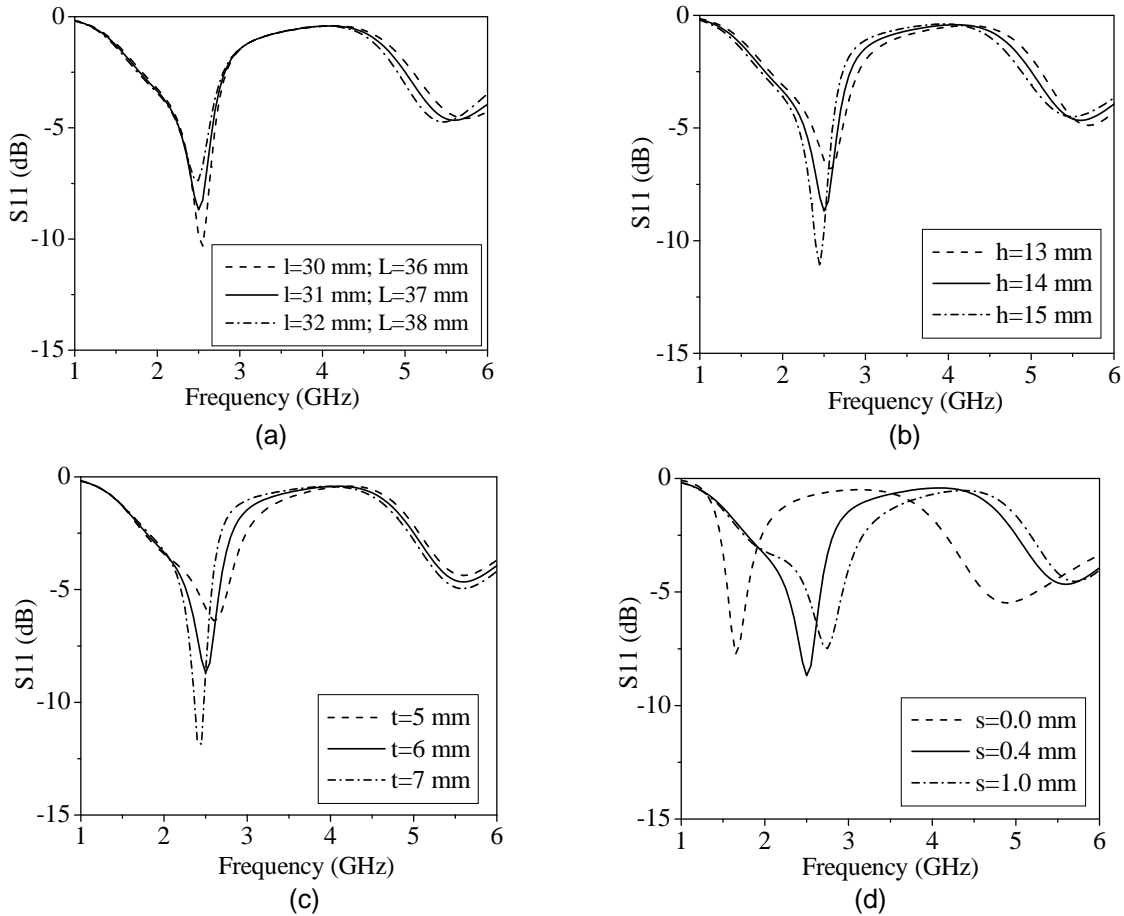


FIGURE 2: Effects of (a) length l , (b) height h , (c) tap distance t and (d) spacing s on the return loss as a function of frequency on the antenna structure of Figure 1(a).

For the analysis of the accuracy optimum segmentation of each geometrical parameter are used in NEC. Figure 1 (a) represents the basic geometry of the IFA. Here one leg of IFA directly connected to the feeding and another leg spaced s from the ground plane. For the simulation we consider portable circuit board (PCB) with permittivity of $\epsilon_r = 2.2$ and substrate thickness of 1.58 mm. The antenna is assumed to feed by 50 Ω coaxial connector, with its central conductor connected to the feeding point and its outer conductor soldered to the ground plane just across the feeding point. In the analysis the dimensions of the ground plane considered as 60 mm \times 60 mm.

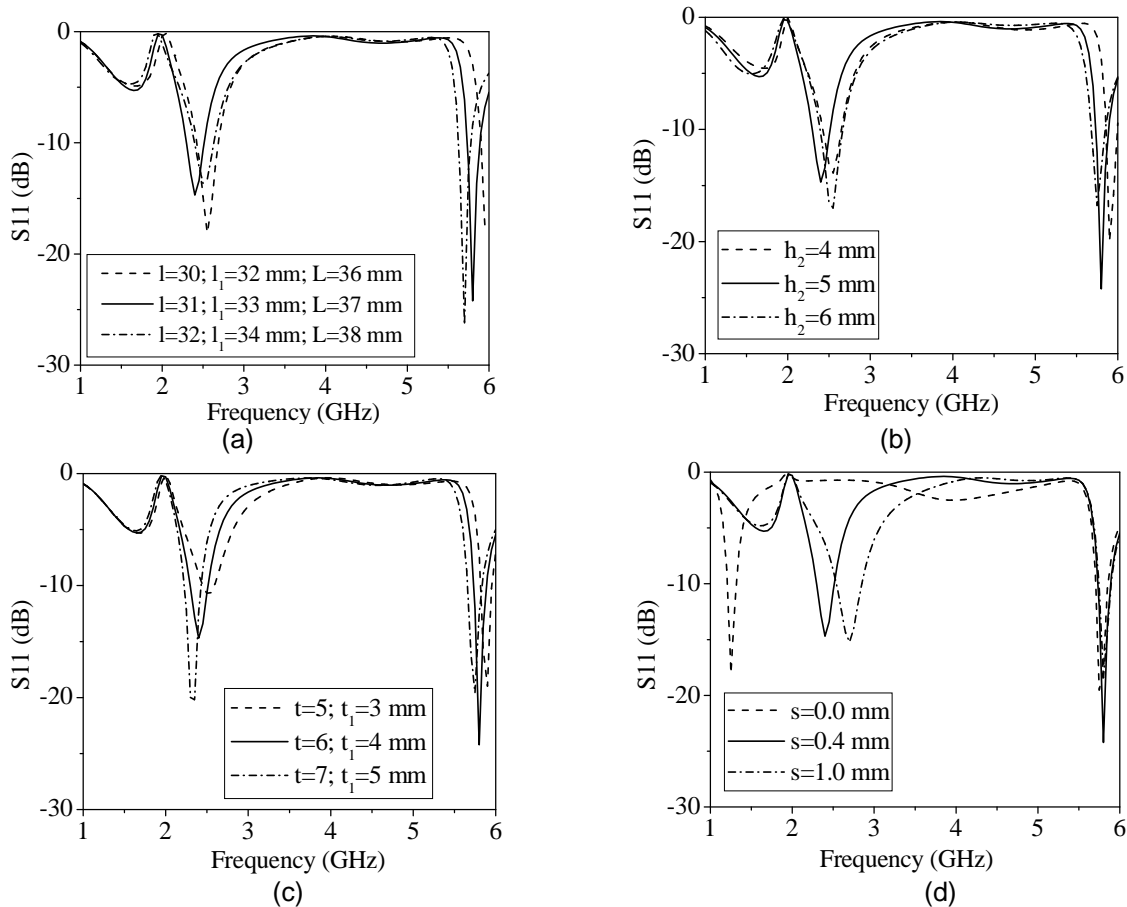


FIGURE 3: Effects of (a) length l , (b) height h_2 , (c) tap distance t and (d) spacing s on the return loss as a function of frequency on the antenna structure of Figure 1(b).

Figure 2 (a) and (b) shows the effects of L and h on the performance of IFA (antenna structure of Figure 1(a)) and Figure 2(c) and (d) represents the effects of t and s on the return loss (S11) of the antenna. Variation of return loss with frequency is like dual band shape but both band stay above the required 10 dB level. From the simulated results, antenna has stable dual shaped bandwidth at $L=l+t=37$ mm and $h=14$ mm. As the performance of IFA is not satisfactory for the multiband operation then we apply a small suitable structured load on the horizontal branch of the IFA named slightly loaded IFA as shown in Figure 1 (b). On the other hand, increase in t causes increase in S11 and narrowing the bandwidth whereas the increase in s causes shift of resonance to the higher frequency. We observe that when we apply that load then the antenna performance improves significantly. We further analysis on the slightly loaded IFA for achieving the structure of best performance. Figure 3 (a) and (b) shows the effects of L and h_2 on the performance of slightly loaded IFA (antenna structure of Figure 1(b)) while Figure 3(c) and (d) represents the effects of t and s on S11. From figure 3 (a) and (b) we observe that a higher value of L or h_2 shifts the antenna resonance to the lower frequencies and a lower value of L or h_2 shifts the antenna resonance to the higher frequencies at upper frequency band and for both lower and

higher value of L and h_2 antenna resonance shifts to the higher frequencies at lower band. Also, change in t for the antenna of structure Figure 1 (b) affect the S11 at lower and upper band. Increase in t results change in resonance from lower to upper frequency while change in s change the resonance as well as maximum values of S11 and mainly it affects the lower resonance band and has smaller effect on upper return loss bandwidth. From the simulation, the optimum dimensions of L and h_2 of slightly loaded IFA are $L=l+t=l_1+t_1=37$ mm and $h_2=5$ mm. From Figure 3 (a) and (b) we also observe that though the return loss of lower band is just below the 10 dB level. But more negative value of antenna return loss means more effectively power transmitted by the antenna in electromagnetic form into free space.

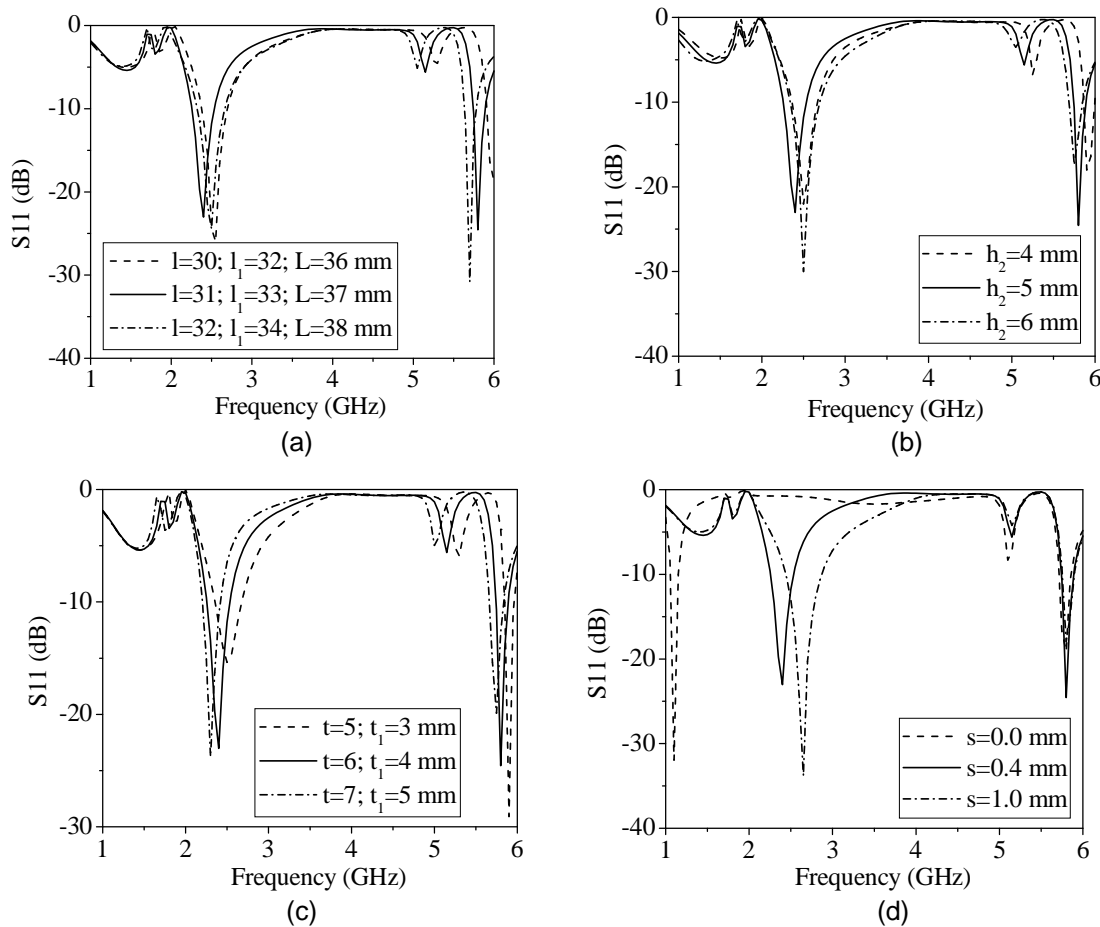


FIGURE 4: Effects of (a) length l , (b) height h_2 , (c) tap distance t and (d) spacing s on the return loss as a function of frequency on the antenna structure of Figure 1(c).

So we further trying to improve the return loss level for the lower frequency band. We observe that when we apply a small load on the horizontal branch of slightly loaded IFA named as moderately loaded IFA shown in Figure 1 (c), the return loss level of lower band improves significantly remaining the return loss level of upper band almost unchanged. Then we tried to find the suitable structure for moderately loaded IFA which provide the best performance for multiband operation. Figure 4 (a) and (b) shows the effects of L and h_2 and Figure 4 (c) and (d) represents the effects of tap distance, t and spacing, s on the performance of moderately loaded IFA (antenna structure of Figure 1(c)). In case of moderately loaded IFA tap distance has not significant effect and does not responsible for causes change in S11 significantly. But change of spacing has significant influence on S11 at lower return loss bandwidth. Zero spacing generate resonance at 1.1 GHz, 0.4 mm spacing shifts the resonance from 1.1 GHz to 2.4 GHz; on the other hand 1 mm spacing shift this resonance to higher frequency and is the order of 2.6 GHz.

While the change in spacing causes no change in return loss bandwidth in the upper band. Thus for slightly loaded and moderately loaded IFA, spacing has no significant effect on the upper operating band but has a great influence on the lower band. Under no load condition spacing has significant effect on the performance of IFA in both lower and upper band. From figure 4 (a) and (b) we observe that a higher value of L or h_2 shifts the antenna resonance to the lower frequencies and a lower value of L or h_2 shifts the antenna resonance to the higher frequencies at upper frequency band, and for both lower and higher value of L and h_2 antenna resonance shifts to the higher frequencies at lower band. From the simulation, the optimum dimensions of L and h_2 of slightly loaded IFA are $L=l+t+l_1+t_1=37$ mm and $h_2=5$ mm. Table 1 represents the optimized numerical value of geometric parameters of the antennas of Figure 1.

TABLE 1: Dimensions of the antennas.

Antenna Name	Antenna Parameters	Values (mm)	Dimension (mm ²)
IFA	l	31	14 × 37
	t	6	
	h	14	
	h_1	13.6	
	w	2	
	s	0.4	
SLIFA (Proposed)	l	31	24 × 37
	l_1	33	
	t	6	
	t_1	4	
	h	14	
	h_1	13.6	
	h_2	5	
	w	2	
MLIFA (Proposed)	l	31	29 × 37
	l_1	33	
	L	37	
	t	6	
	t_1	4	
	h_1	13.6	
	h_2	5	
	w	2	
	s	0.4	

3. NUMERICAL SIMULATION RESULTS

The simulated return losses of IFA (geometry of Figure 1 (a)), proposed slightly loaded (geometry of Figure 1 (b)) and moderately loaded (geometry of Figure 1 (c)) IFA are shown in Figure 5. From the simulation results, the slightly loaded IFA has return loss bandwidth of 235 MHz (frequency ranges 2285 – 2520 MHz) at lower operating band and 150 MHz (frequency ranges 5730 – 5880 MHz) at upper operating band. The lower operating band covers the 100 % of 2.3 GHz mobile WiMAX (2.3 – 2.4 GHz) operating band and 2.4 GHz IEEE 802.11b/g WLAN/Bluetooth (2.4 – 2.5 GHz) operating band. On the other hand, at the upper return loss bandwidth of the antenna of geometry of Figure 1(b) cover the 97 % of 5.8 GHz Wi-Fi (frequency ranges 5725 – 5875 GHz) operating band. Due to the increase in load to the IFA, the modified moderately loaded IFA has improved return loss than antenna of structure 2 (geometry of Figure 1(b)). Moderately loaded IFA has lower band return loss bandwidth of 270 MHz (2260 – 2530 MHz) which fully occupy the 2.3 GHz Mobile WiMAX and 2.4 GHz Bluetooth/WLAN operating band. Moreover, the upper band bandwidth of 150 MHz (5735 – 5885 MHz) covers 93 % of 5.8 GHz Wi-Fi operation. The variations of voltage standing wave ratio (VSWR) as a function of frequency are shown in Figure 6 for both all operating bands. From the obtained results, as the

load applied to the IFA, the VSWR improves significantly and appear close to standard value 1 in both antenna return loss bandwidth.

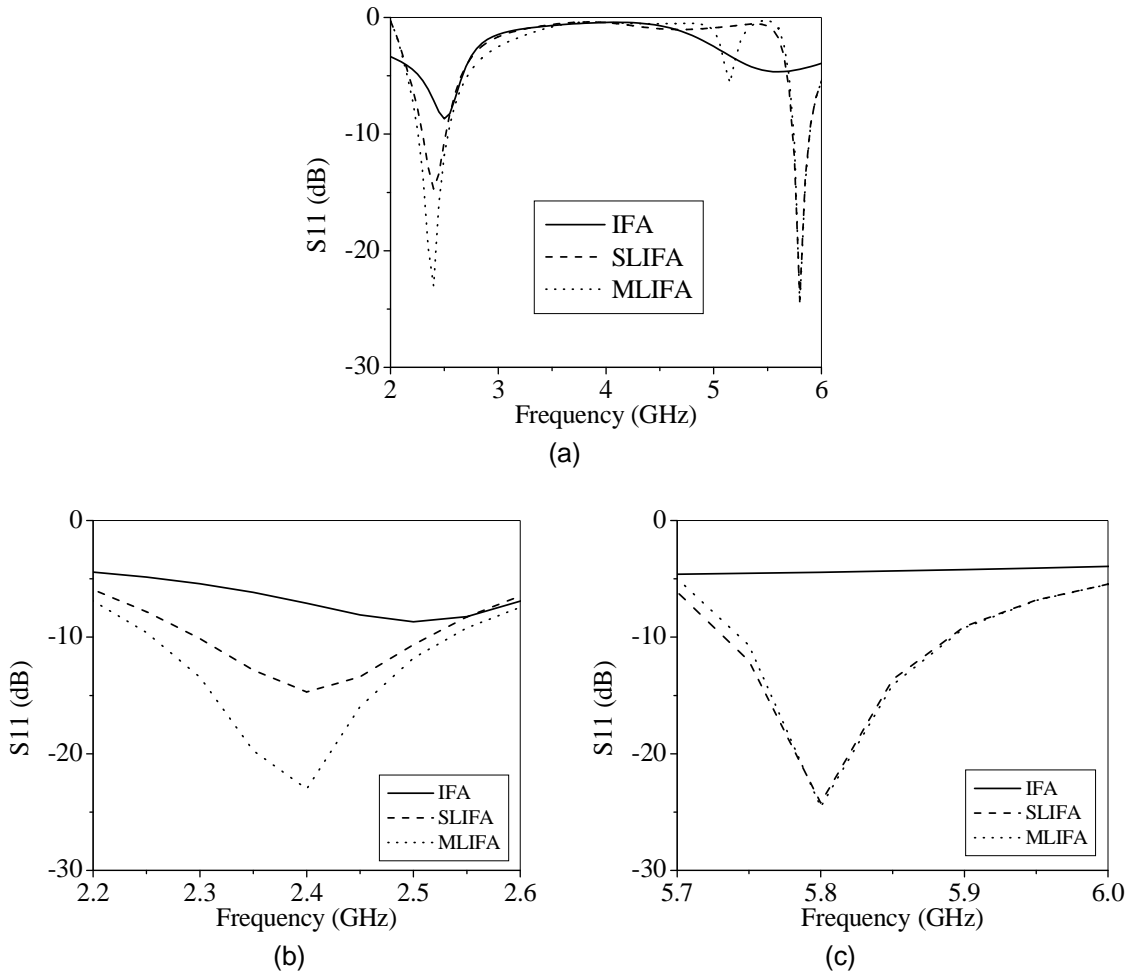


FIGURE 5: Antennas return loss (a) as a function of frequency (b) lower return loss bandwidth and (c) upper return loss bandwidth.

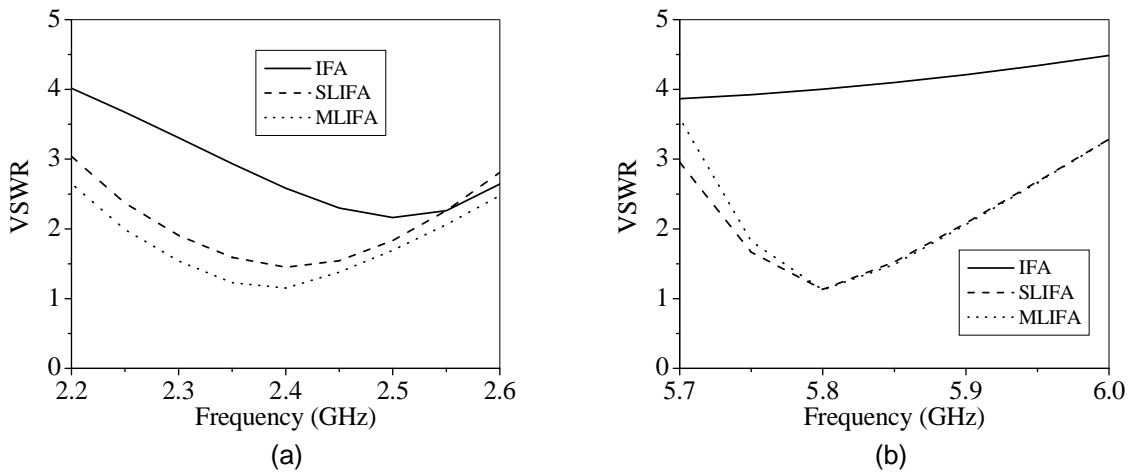


FIGURE 6: Variation of VSWR of the antennas of geometry of Figure 1, as a function of frequency at (a) lower return loss bandwidth and (b) upper return loss bandwidth.

Figure 7 represents the antennas input impedance variation and Figure 8 represents the antennas phase shift causes due the impedance mismatch as a function of frequency. From the obtained results, structure 3 (moderately loaded IFA) has much better antenna input impedance than rest two structures (structure 1 and 2). Also, from the simulation study, the phase shift decrease with the application of load to the IFA.

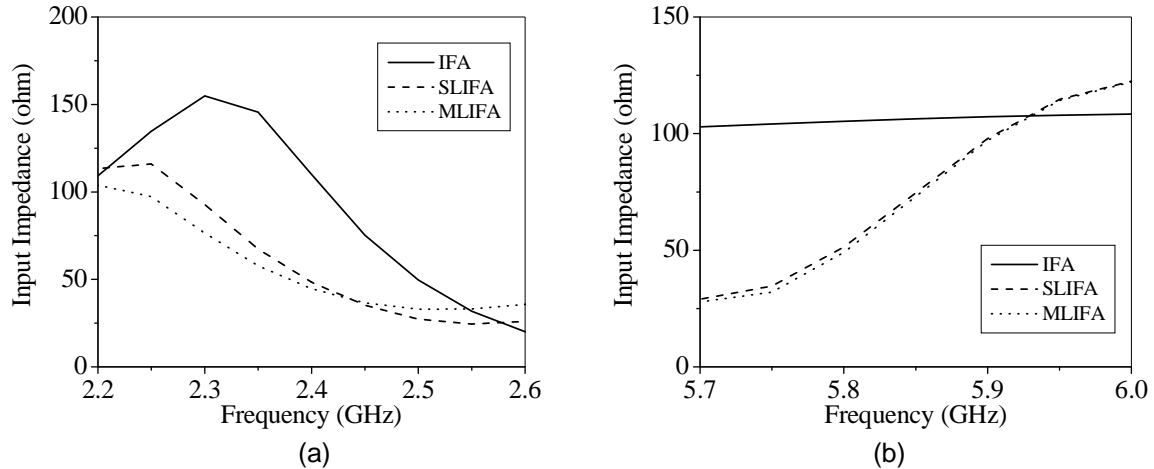


FIGURE 7: Input impedance variation of the antennas of Figure 1 with respect to the frequency at (a) lower return loss bandwidth and (b) upper return loss bandwidth.

The antennas gain variation as a function of frequency is shown in Figure 9. From the obtained results, antenna gain varies 6.91 to 8.95 dBi at within 2.25 GHz to 2.55 GHz for the IFA (geometry structure 1), 8.04 to 8.97 dBi for slightly loaded IFA (geometry structure 2) and 8.3 to 8.65 dBi for moderately loaded IFA (geometry structure 3). And within the upper return loss bandwidth (frequency 5.7 – 5.9 GHz) the gain varies from 2.79 to 2.56 dBi, from 6.98 to 4.69 dBi, and from 7.61 to 5.18 dBi for the IFA, slightly loaded IFA and moderately loaded IFA respectively.

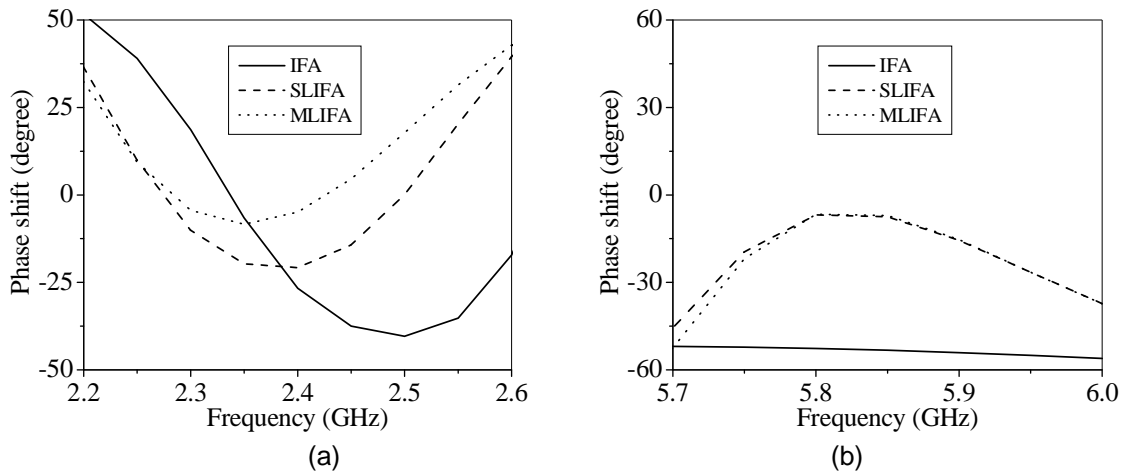


FIGURE 8: Phase shift of the antenna as a function of frequency at (a) lower return loss bandwidth and (b) upper return loss bandwidth.

Peak gain comparison with the proposed antenna and reference antenna for mobile WiMAX, Wi-Fi, WLAN and Bluetooth application are listed in Table 2. From the comparison table, proposed loaded IFA's has much higher gain than the antenna have been proposed for mobile WiMAX, Bluetooth, WLAN and Wi-Fi operation.

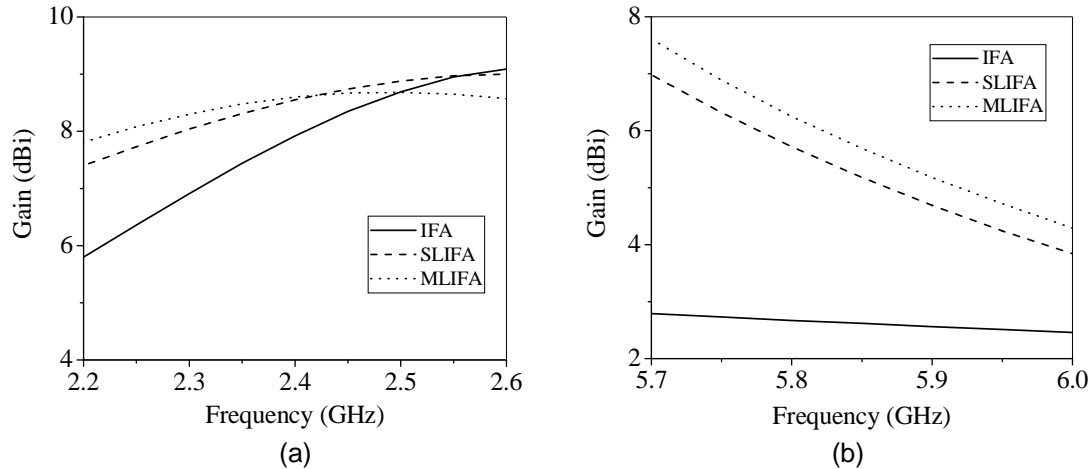


FIGURE 9: Variation of antenna gain as a function of frequency at (a) lower return loss bandwidth and (b) upper return loss bandwidth.

TABLE 2: Gain comparison between the proposed and reference antennas.

Antenna	Gain (dBi)		
	2.3 GHz mobile WiMAX	2.4 GHz WLAN or Bluetooth	5.8 GHz Wi-Fi
Slightly loaded IFA (structure 2)	8.31	8.88	6.32
Moderately loaded IFA (structure 3)	8.48	8.67	6.89
Compact monopole antenna [1]	-	1.35	2.10
Printed multiband antenna [11]	-	-3.1	3.21
Printed monopole array antenna [12]	-	3.4	6.4
T-shaped monopole with shorted L-shaped strip sleeves antenna [13]	-	3.4	1
Microstrip coupled printed PIFA [14]	-	4.2	6.4
Surface mount monopole antenna [15]	-	4.3	5.1
CPW-fed triangular shaped monopole antenna [17]	-	2.14	3.05
Metal plate antenna [18]	2.12	2.5	4.8
Composite monopole antenna [19]	-	2.3	4.8
Compact loop antenna [21]	-	2.63	5.48
Flat plate antenna with shorted parasitic element [23]	-	2.8	5.48

Figure 10 (a) and (b) represents the normalized radiation pattern of the antenna of Figure 1(b) (slightly loaded IFA) for 2.4 GHz resonant frequency of total gain in vertical plane (XZ, YZ plane) and horizontal plane (XY plane) respectively. Figure 10 (c) and (d) represents the normalized horizontal gain in horizontal plane and normalized vertical gain in horizontal plane respectively for slightly loaded IFA. Also, the normalized total gain pattern of the antenna at 5.8 GHz in vertical plane (XZ, YZ plane) and horizontal plane (XY plane) are shown in Figure 11 (a) and (b). Moreover, Figure 11 (c) and (d) represents the normalized horizontal gain in horizontal plane (XY plane) and normalized vertical gain in horizontal plane (XY plane) respectively at 5.8 GHz. From the obtained radiation pattern, the slightly loaded IFA has good radiation characteristics in both planes at both operating frequencies. Combining all radiation, it seems to be a half-orange shape with very high gain. Figure 12 (a) and (b) represents the normalized total gain pattern of moderately loaded IFA (antenna of Figure 1(c)) in XZ/YZ and XY plane at 2.4 GHz frequency and the normalized total gain pattern for 5.8 GHz are shown in Figure 13 (a) and (b) for XZ/YZ and XY planes. Figure 12 (c) and (d) presents the normalized horizontal and vertical gain in XY plane at 2.4 GHz while Figure 13 (c) and (d) shows the normalized horizontal and vertical gain in XY plane at 5.8 GHz for moderately loaded IFA. From the obtained radiation patter for this antenna, it has acceptable radiation characteristics in all planes (XY, YZ, ZX) at both operating frequencies (lower and upper band).

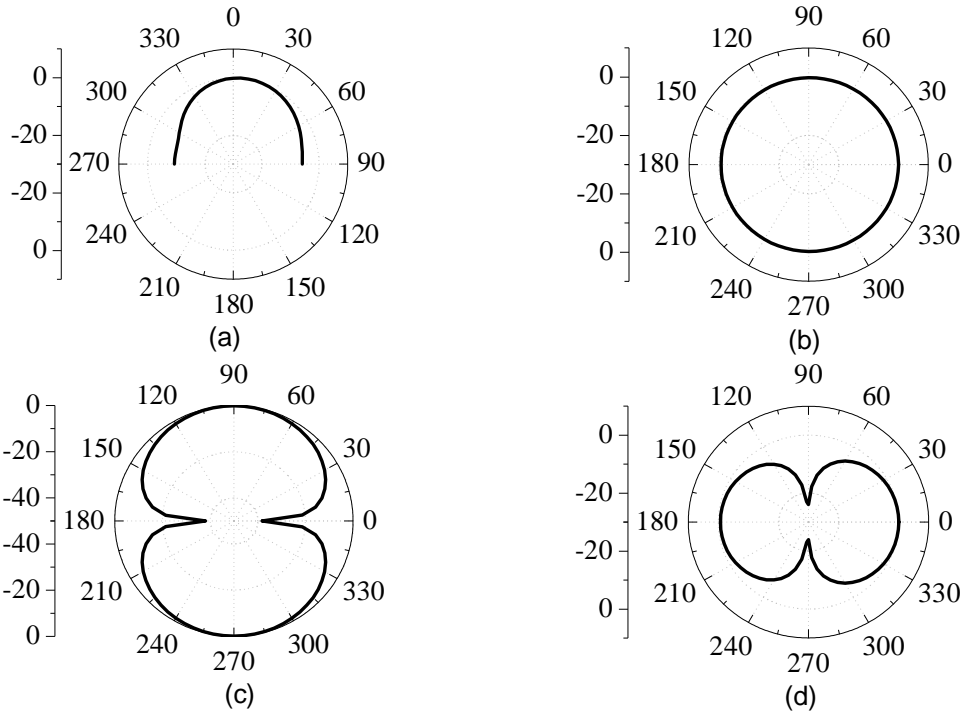


FIGURE 10: Radiation pattern (normalized) of slightly loaded IFA (antenna geometry of Figure 1(b)) at 2.4 GHz: (a) total gain in vertical plane (XZ, YZ), (b) total gain in horizontal plane (XY), (c) horizontal gain horizontal plane (XY) and (d) vertical gain horizontal plane (XY).

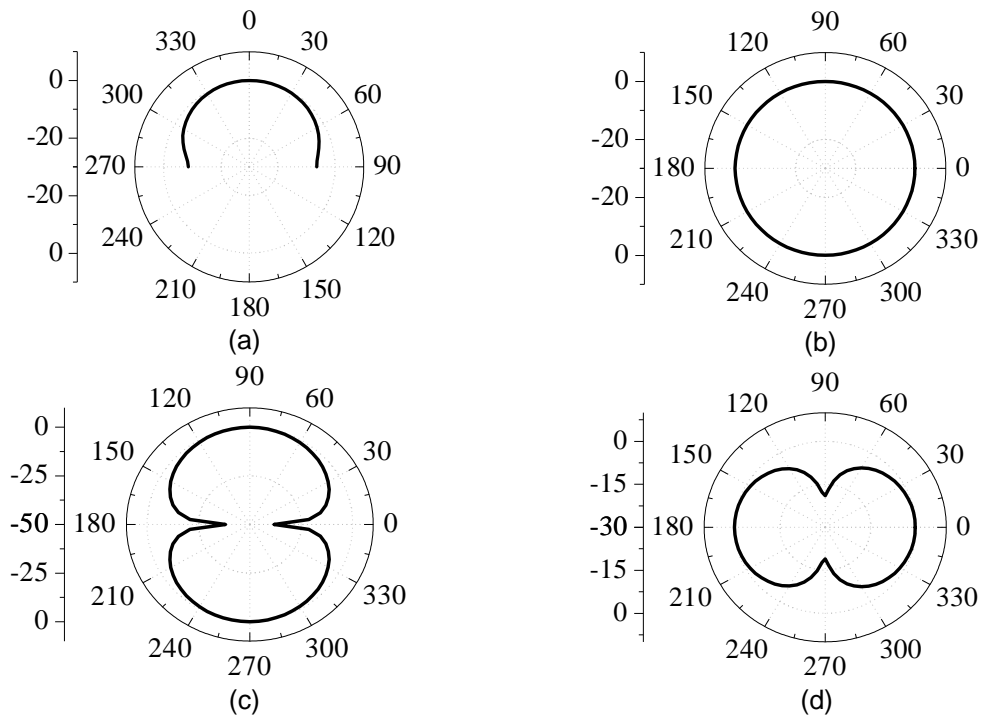


FIGURE 11: Radiation pattern (normalized) of slightly loaded IFA (antenna geometry of Figure 1(b)) at 5.8 GHz: (a) total gain in vertical plane (XZ, YZ), (b) total gain in horizontal plane (XY), (c) horizontal gain horizontal plane (XY) and (d) vertical gain horizontal plane (XY).

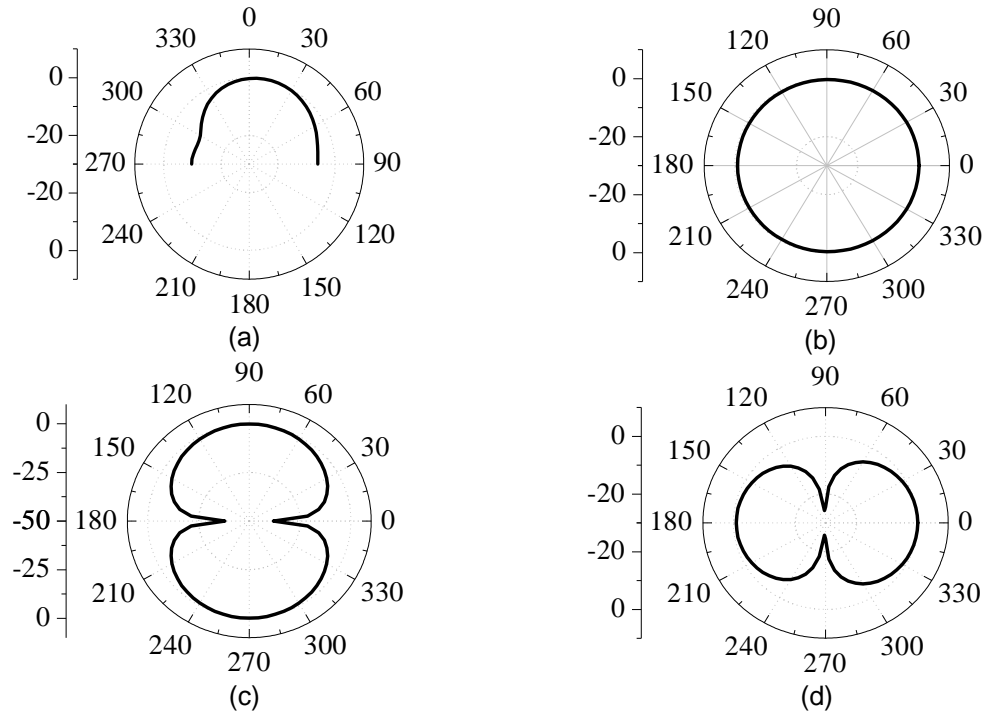


FIGURE 12: Radiation pattern (normalized) of moderately loaded IFA (antenna geometry of Figure 1(c)) at 2.4 GHz: (a) total gain in vertical plane (YZ, XZ), (b) total gain in horizontal plane (XY), (c) horizontal gain horizontal plane (XY) and (d) vertical gain horizontal plane (XY).

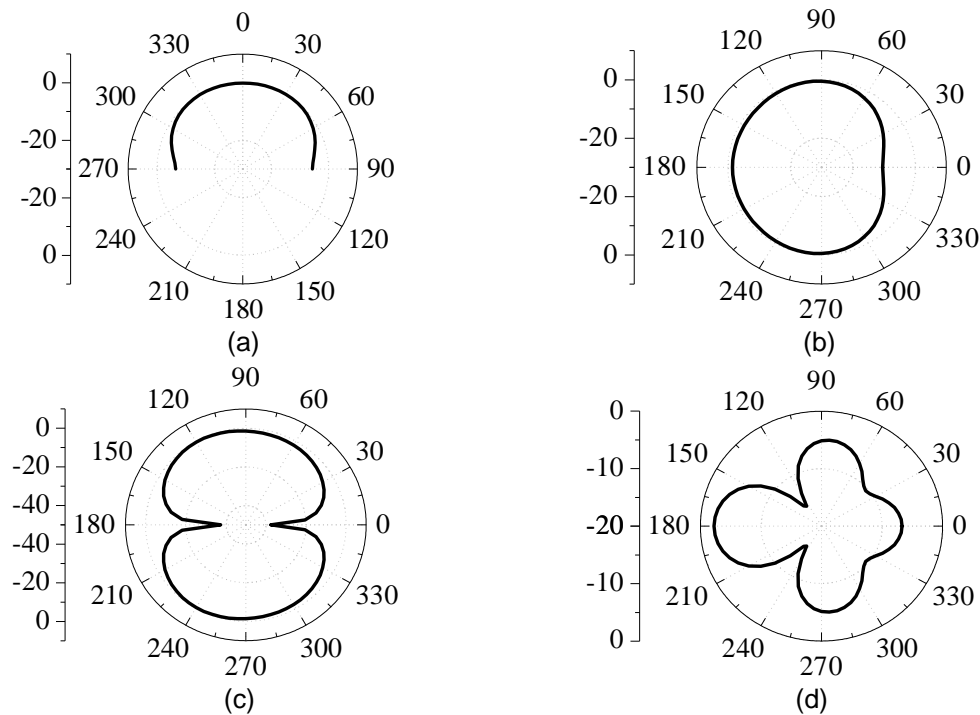


FIGURE 13: Radiation pattern (normalized) of moderately loaded IFA (antenna geometry of Figure 1(c)) at 5.8 GHz: (a) total gain in vertical plane (YZ, XZ), (b) total gain in horizontal plane (XY), (c) horizontal gain horizontal plane (XY) and (d) vertical gain horizontal plane (XY).

4. CONCLUSION & FUTURE WORK

Multiband slightly and moderately loaded inverted-F antennas have been proposed and analyzed by means of numerical simulations using MOM's in NEC. The antennas geometry analyzed by varying the four major geometry parameters (length, height, tap distance and spacing). For both antennas, spacing has significant influence on the lower operating band while it has negligible effect on the upper band. From the four parameters analysis antenna geometry chosen and proposed antennas performance parameters are analyzed for multiband operations. The proposed antennas have high gain for mobile WiMAX, WLAN, Bluetooth and Wi-Fi operation. It is also observed that improvements in antenna gain, input impedance, phase shift and return loss have been obtained when structured load is applied to the IFA. The antennas are of small size and good radiation characteristics. Due to the compact area occupied, the proposed antennas are promising to be embedded within the different mobile devices employing mobile WiMAX, Wi-Fi, Bluetooth and WLAN operation.

Our future target is miniaturization of the proposed antennas with increasing operating bandwidth and gain.

5. REFERENCES

- [1] J. Jung, H. Lee and Y. Lim. "Compact Monopole Antenna for Dual ISM-Bands (2.4 and 5.8 GHz) Operation". *Microwave and Optical Technology Letters*, 51(9): 2227-2229, 2009
- [2] K. -L. Wong and P. -Y. Lai. "Wideband Integrated Monopole Slot Antenna for WLAN/WiMAX Operation in the Mobile Phone". *Microwave and Optical Technology Letters*, 50(8): 2000-2005, 2008
- [3] W. C. Liu and W. R. Chen. "CPW-Fed Compact Meandered Patch Antenna for Dual-Band Operation". *Electronics Letters*, 40(18): 1094-1095, 2004
- [4] T. H. Kim and D. C. Park. "CPW-Fed Compact Monopole Antenna for Dual-Band WLAN Applications". *Electronics Letters*, 41(6): 292-293, 2005
- [5] Y. -D. Lin and P. -L. Chi. "Tapered Bent Folded Monopole for Dual-Band Wireless Local Area Network (WLAN) Systems". *IEEE Antennas and Wireless Propagation Letters*, 4: 355-357, 2005
- [6] Y. -L. Kuo and K. -L. Wong. "Printed Double-T Monopole Antenna for 2.4/5.2 GHz Dual-Band WLAN Operations". *IEEE Transactions on Antennas and Propagation*, 51(9): 2187-2192, 2003
- [7] S. H. Choi, J. K. Park, S. K. Kim and H. Y. S. Kim. "Design of Dual-Band Antenna for the ISM Band Using a Backed Microstrip Line". *Microwave and Optical Technology Letters*, 41(6): 457-460, 2004
- [8] C. -Y. Huang and P. -Y. Chiu. "Dual-Band Monopole Antenna with Shorted Parasitic Element". *Electronics Letters*, 41(21): 1154-1155, 2005
- [9] M. N. Suma, R. K. Raj, M. Joseph, P. C. Bybi and P. Mohanan. "A Compact Dual-Band Planar Branched Monopole Antenna for DCS/2.4 GHz WLAN Applications". *IEEE Microwave and Wireless Components Letters*, 16(5): 275-277, 2006
- [10] C. -Y. Pan, T. -S. Horng, W. -S. Chen and C. -H. Huang. "Dual Wideband Printed Monopole Antenna for WLAN/WiMAX Applications". *IEEE Antennas and Wireless Propagation Letters*, 6: 149-151, 2007

- [11] S. -Y. Sun, S. -Y. Huang and J. -S. Sun. "A Printed Multiband Antenna for Cellphone Applications". *Microwave and Optical Technology Letters*, 51(3): 742-744, 2009
- [12] T. -Y. Wu, S. -T. Fang and K. -L. Wong. "Printed Monopole Array Antenna for WLAN Operation in the 2.4/5.2/5.8 GHz Bands". *Microwave and Optical Technology Letters*, 37(5): 370-372, 2003
- [13] J. -W. Wu, Y. -D. Wang, H. -M. Hsiao and J. -H. Lu. "T-Shaped Monopole Antenna with Shorted L-Shaped Strip-Sleeves for WLAN 2.4/5.8-GHz Operation". *Microwave and Optical Technology Letters*, 46(1): 65-69, 2005
- [14] K. -L. Wong and W. -J. Chen. "Small-Size Microstrip-Coupled Printed PIFA for 2.4/5.2/5.8 GHz WLAN Operation in the Laptop Computer". *Microwave and Optical Technology Letters*, 51(9): 2072-2076, 2009
- [15] S. -W. Su, S. -T. Fang and K. -L. Wong. "A Low-Cost Surface-Mount Monopole Antenna for 2.4/5.2/5.8-GHz Band Operation". *Microwave and Optical Technology Letters*, 36(6): 487-489, 2003
- [16] L. Pazin, N. Telzhensky and Y. Leviatan. "Multiband Flat-Plate Inverted-F Antenna for Wi-Fi/WiMAX Operation". *IEEE Antennas and Wireless Propagation Letters*, 7: 197-200, 2008
- [17] Y. Song, Y. -C. Jiao, G. Zhao and F. -S. Zhang. "Multiband CPW-Fed Triangle-Shaped Monopole Antenna for Wireless Applications". *Progress in Electromagnetics Research, PIER*, 70: 329–336, 2007
- [18] K. -L. Wong and L. -C. Chou. "Internal Wideband Metal-Plate Antenna for Laptop Application". *Microwave and Optical Technology Letters*, 46(4): 384-387, 2005
- [19] K. -L. Wong and L. -C. Chou. "Internal Composite Monopole Antenna for WLAN/WiMAX Operation in A Laptop Computer". *Microwave and Optical Technology Letters*, 48(5): 868-871, 2006
- [20] C. -J. Wang and S.-W. Chang. "Studies on Dual-Band Multi-Slot Antennas". *Progress in Electromagnetics Research, PIER*, 83: 293–306, 2008
- [21] Y. -S. Shin and S. -O. Park. "A Compact Loop Type Antenna for Bluetooth, S-DMB, WiBro, WiMAX, and WLAN Applications". *IEEE Antennas and Wireless Propagation Letters*, 6: 320-323, 2007
- [22] Y. -S. Shin and S. -O. Park. "A novel compact PIFA for Wireless Communication applications". *IEEE Region 10 Conference*, 2007
- [23] K. -L. Wong, L. -C. Chou and C. -M. Su. "Dual-Band Flat-Plate Antenna with a Shorted Parasitic Element for Laptop Applications". *IEEE Transactions on Antennas and Propagation*, 53(1): 539-544, 2005
- [24] Wei-Cheng Su and Kin-Lu Wong. "Internal PIFA's for UMTS/WLAN/WiMAX Multi-Network Operation for a USB Dongle". *Microwave and Optical Technology Letters*, 48(11): 2249-2253, 2006
- [25] Y. -S. Wang, M. -C. Lee and S. -J. Chung. "Two PIFA-Related Miniaturized Dual-Band Antennas". *IEEE Transactions on Antennas and Propagation*, 55(3): 805-811, 2007

- [26] K. L. Chung, T. H. Mak and W. Y. Tam. "A Modified Two-Strip Monopole Antenna for Wi-Fi and WiMAX Applications". *Microwave and Optical Technology Letters*, 51(12): 2884-2886, 2009
- [27] K. -L. Wong, T. -Y. Wu, S. -W. Su and J. -W. Lai. "Broadband Printed Quasi-Self-Complementary Antenna for 5.2/5.8 GHz WLAN Operation". *Microwave and Optical Technology Letters*, 39(6): 495-496, 2003
- [28] W. -C. Liu. "A Coplanar Waveguide-Fed Folded-Slot Monopole Antenna for 5.8 GHz Radio Frequency Identification Application". *Microwave and Optical Technology Letters*, 49(1): 71-74, 2007
- [29] W. -C. Liu and C. -M. Wu. "CPW-Fed Shorted F-Shaped Monopole Antenna for 5.8-GHz RFID Application". *Microwave and Optical Technology Letters*, 48(3): 573-575, 2006
- [30] Z. N. Chen and M. Y. W. Chia. "Broadband Planar Inverted-L Antennas". *IEE Proceedings Microwave Antennas Propagation*, 148(5): 339-342, 2001
- [31] S. -W. Su, K. -L. Wong and H. -T. Chen. "Broadband Low-Profile Printed T-Shaped Monopole Antenna for 5-GHz WLAN Operation". *Microwave and Optical Technology Letters*, 42(3): 243-245, 2004
- [32] G. J. Burke and A. J. Poggio. "Numerical Electromagnetic Code-2". Ver. 5.7.5, Arie Voors, 1981
- [33] M. -C. T. Huynh. "A Numerical and Experimental Investigation of Planar Inverted-F Antennas for Wireless Communication Applications". M.Sc. Thesis, Virginia Polytechnic Institute and State University, October 2000
- [34] K. Hirisawa and M. Haneishi. "Analysis, Design, and Measurement of small and Low-Profile Antennas". Artech House, Boston, 1992

Solution algorithms for a deterministic replacement problem

Zakir H. Ahmed

*Department of Computer Science,
Al-Imam Muhammad Ibn Saud Islamic University,
P.O. Box No. 5701, Riyadh-11432
Kingdom of Saudi Arabia*

zhahmed@gmail.com

Abstract

We consider the life of a k -series system with $n-k$ standbys, which are to replace the working items as they fail in a specified order. Also the life of each item is assumed to be known. The problem is to find the first k elements to be used in the system to start with and the sequence in which replacements are to be made such that the system life is maximized. It is pointed out that this problem is essentially a 'bottle-neck' problem in that it is equivalent to partitioning n numbers into k subsets (parts) such that the minimum of the k part-sums is maximized. Effective bounds can be computed for the optimum solution value and this can be used to develop an efficient lexisearch algorithm for optimization. Also the paper develops a genetic algorithm which gives heuristically optimal solution to the problem. The efficiency of the genetic algorithm to the 'bottle-neck' maximin problem as against lexisearch algorithm has been examined for some randomly generated instances of different sizes.

Keywords: Deterministic replacement, bottleneck, lexisearch, genetic algorithms.

1. INTRODUCTION

In reliability engineering, the k -out-of- n series system is an important system as most systems can be modeled as series system. It is defined to a complex coherent system with n independent components such that the system operates if and only if at least k of these components function successfully. For a complex and expensive system, it may not be advisable to replace the system just because of the failure of one component. In fact, the system re-operates on repair or replacement of the failed component by a new one. Such replacement does not renew the system, but enable the system to continue to operate. So, the system can re-operate as long as number of failed components does not exceed $n-k$. However, once the number of failed components surpasses $n-k$, the system does not re-operate [16]. This system is also referred as a series system with standbys [10, 14].

There are many application of the system, such as process and energy system, transport system, bridges, pipelines, space shuttles, etc. Reliability, availability and maintenance model of the system have been studied in the reliability literature [10, 14, 15, 16]. There are some literatures on this, but with group replacement, which is referred as opportunity based maintenance [11]. Savic et al. [13] have proved that this opportunistic problem is NP-complete, and developed genetic algorithm for analyzing this optimal opportunistic problem for real-sized systems. They analyzed different operators using a system that consists of 50 maintenance significant parts, and paid special attention to the sensitivity of solutions to the maximum number of maintenance group. A dynamic opportunistic maintenance policy for continuously monitored system has been proposed [17]. An opportunistic maintenance policy for a multi-component damage shock model with stochastically dependent components was proposed [5]. Zhaou et al. [18] introduced an opportunistic preventive maintenance (PM) scheduling algorithm based on dynamic programming for the multi-unit series system. A genetic algorithm for time and cost analysis for a Potash industry has been developed to build an intelligent maintenance system to predict whether the opportunity based maintenance strategy is cost effective or not [12].

We consider the problem as optimization of the component replacement sequence when the data is

deterministic and replacement is single. Of course, we do not consider the replacement cost or time. We show that the system is equivalent to a ‘bottleneck-maximin’ problem, of partitioning a set of n numbers into k parts, such that the minimum of the k part-sums is maximized. A preliminary study was carried out by Ahmed et al. [4]. It is a combinatorial optimization problem in nature. An interesting feature of combinatorial optimization problems is that it may be easy to hit upon the optimal solution but in contra-distinction to the ‘continuous’ mathematical programming problems, it is almost impossible to identify it as such by ‘general methods’. No necessary conditions, let alone necessary and sufficient conditions, for a solution to be optimal, of the usual type (like the derivatives being zero) are available. However, it often happens that efficient bounds to optimal value (either globally or over well-defined subsets of the set of solutions) can be found, making possible non-trivial statements about the ‘goodness’ of a proposed solution. In fact, this possibility is at the heart of search algorithms like the lexisearch [2, 3, 9] and branch and bound [8] algorithms. In this paper, we are going to develop a lexisearch algorithm to find exact optimal solution and a genetic algorithm to find heuristic solution to the problem.

The paper is organized as follows: Section 2 gives a detailed statement of the problem. A lexisearch algorithm is applied in Section 3 to find exact optimal solution to the problem. Section 4 develops a genetic algorithm for the same. Section 5 describes computational experience for the algorithms. Finally, Section 6 presents comments and concluding remarks.

2. STATEMENT OF THE PROBLEM

Let $S_0 = \{C_1, C_2, \dots, C_n\}$ be a set of n components or elements, with corresponding lives $\{t_1, t_2, \dots, t_n\}$. A system requires k of these elements for it to be in operation. Thus initially one has k components put to work in the system, keeping the remaining n-k components as standbys, to replace ‘active elements’ in the system, sequentially, as and when they fail. The objective is to choose the initial set of active elements and the sequence in which the standby elements are to replace the elements on failure, so that the system life is maximized.

2.1. Illustration

Let C_i , ($i = 1, 2, 3, \dots, 8$) be 8 components, with lives $\{t_i, i=1, 2, \dots, 8\} = \{4, 7, 8, 9, 10, 15, 15, 20\}$ in suitable time units. Let $k=3$ and the replacement sequence be $\{C_1, C_2, C_3; C_4, C_5, \dots, C_8\}$. That is, one starts with the three items C_1, C_2, C_3 , with lives 4, 7 and 8 respectively, in the system, and as the active items fail, they are replaced by the items with lives 9, 10, 15, 15 and 20 in that order. The sequence of failures/ replacements can be schematically represented as shown in Table 1.

Stage No.	Cumulative time till failure	Time to failure	Active element life in respective points of failure	Lives of ordered set of standbys
0	0	0	4(C_1), 7(C_2), 8(C_3)	9, 10, 15, 15, 20
1	4	4	9*(C_4), 3(C_2), 4(C_3)	10, 15, 15, 20
2	7	3	6(C_4), 10*(C_5), 1(C_1)	15, 15, 20
3	8	1	5(C_4), 9(C_5), 15*(C_6)	15, 20
4	13	5	15*(C_7), 4(C_5), 10(C_6)	20
5	17	4	11(C_7), 20*(C_8), 6(C_6)	*
6	23	6	5(C_7), 14(C_8), 0(C_6)	

TABLE 1: The sequence of failures / replacements

Starting with C_1, C_2 and C_3 , we find that C_1 fails first, at time $t = 4$, to be replaced by C_4 ; with $t_4 = 9$. Now C_2, C_3 and C_4 have 3, 4 and 9 units of time left for failure and the four items C_j , ($j= 5, 6, 7$ and 8) with life 10, 15, 15, 20 are the ordered spares. The process is continued till the system fails totally. For the sequence (1, 2, ..., 8), the system breakdown time is 23 time units. The same set of units, with different orders of replacement, leads to different system lives. For instance, the sequence (5, 1, 3, 6, 4, 8, 2, 7) gives a system life of 24 units and the sequences (4, 2, 6, 7, 8, 5, 1, 3) and (8, 1, 3, 5, 6, 7, 2, 4) lead to system lives of 26 and 27 units respectively. Our aim is to obtain the maximum system life by choosing an appropriate sequence.

2.2. Bound setting

It is easy to get some good upper bounds to the optimal values of this problem. Two such bounds are given below:

(i) Let $T_0 = \sum_{i=1}^n t_i$. Then, $\alpha_1 = \left\lfloor \frac{T_0}{k} \right\rfloor$ is one such upper bound.

(ii) Let the components be re-labeled, if necessary, such that $t_i \geq t_{i+1}$. Also, let $t_1, t_2, \dots, t_{r_1} \geq \alpha_1$, but $t_{r_1+1} < \alpha_1$. Then,

$$\alpha_2 = \frac{T_0 - \sum_{i=1}^{r_1} t_i}{k - r_1}$$

is also an upper bound. This bounding process can be recursively applied, treating the set $S_1 = S_0 - \{C_i, i = 1, 2, \dots, r_1\}$ as the set to be partitioned into $k_1 = k - r_1$ subsets, where S_0 is the set of all component lives in non-increasing order. Let us illustrate it as below.

(i) Let $S_0 = \{20, 15, 15, 10, 9, 8, 7, 4\}$ and $k=3$. We have $T_0=88$, and then $\alpha_1=29$. Since the sequence $\{20,4,8,10,15,15,9,7\}$ leads to a solution value 27, any improvement, if at all achieved, will be not more than 2 ($=29 - 27$).

(ii) Let $S_0 = \{40, 17, 10, 9, 8, 5\}$ and $k=3$. Then $\alpha_1 = 29$. Hence, $S_1 = \{17, 10, 9, 8, 5\}$ with sum, say $T_1=49$, and $\alpha_2 = 24$ and the best partition of S_1 into two parts is equivalent to the best partition into 3 parts of S_0 . The partition $S_{11}=\{17,8\}$, $S_{12}=\{10,9,5\}$ of S_1 is of value 24 and hence a best partition of S_0 into three parts is $S_{01} = \{40\}$, $S_{02}=\{17,8\}$ and $S_{03}=\{10,9,5\}$, with value 24.

It is worth noting that this problem, formulated as a 'bottleneck' problem in a 'dynamic background' (viz., replacing an item as and when it fails) and thus is one with 'permutations' as the 'variable' over whose domain an objective function is to be maximized, is equivalent to the 'static' problem - of partitioning a set of numbers into k parts such that the minimum among the part sums is maximized. For instance, take the case of the set $\{4, 7, 8, 9, 10, 15, 15, 20\}$, with $k=3$ considered already in Table 1. On examining the failure patterns table vertically with the top entries 4, 7 and 8, one is easily led to the partitions $\{4, 9, 15\} \cup \{7, 10, 20\} \cup \{8, 15\}$, with part sums 28, 37 and 23 and hence the objective function value $23 = \min. \{28, 37, 23\}$. A permutation of these parts within themselves gives rise to a different sequence but give the same objective function value. For instance, consider the following permutation: $\{9, 15, 4\} \cup \{7, 20, 10\} \cup \{15, 8\}$. The sequence is assembled as follows:

Take the first element of each of these parts, to start the system. Whichever is the smallest among them in failure time will fail first; replace it by the next element in the corresponding part. The process is repeated till an element fails but the corresponding part is 'empty'. Details are given in Table 2(a).

Failure time		Partition			Lives of standbys
Cum.	Stage	I	II	III	in the partitions
0	0	9	7	15	$\{15,4\} \cup \{20,10\} \cup \{8\}$
7	7	2	20*	8	$\{15,4\} \cup \{10\} \cup \{8\}$
9	2	15*	18	6	$\{4\} \cup \{10\} \cup \{8\}$
15	6	9	12	8*	$\{4\} \cup \{10\} \cup \{*\}$
23	8	1	4	0	$\{4\} \cup \{10\} \cup \{*\}$

TABLE 2(a): Permutation of parts

Finally the sequence is got, in the above case, as {9, 7, 15; 20, 15, 8, 4, 10}. Obviously, if the columns I, II and III of the Table 2(a) are permuted, along with the 'part-sets', one gets a different sequence which is equivalent to the first, with the same objective function value: Thus, writing the columns as I = III, II = II, and III= I, we get the sequence {15, 7, 9; 20, 15, 8, 4, 10} as in the failure Table 2(b).

Failure time		Partition			Lives of standbys in the partitions
Cum.	Stage	I	II	III	
0	0	15, 7, 9			{8}U{20,10}U{15,4}
7	7	8, 20*, 2			{8}U{10}U{15,4}
9	2	6, 18, 15*			{8}U{10}U{4}
15	6	8*, 12, 9			{*}U{10}U{4}
23	8	0, 4, 1			{*}U{15}U{4}

TABLE 2(b): Permutation of parts

In fact, every partition $n=n_1+n_2+\dots+n_k$ gives rise to $n_1! n_2! \dots n_k!$ permutations of n components, each of which corresponds to a unique failure pattern, all of them giving the same part sums and hence the same objective function value. For instance, the same partition as above, by taking the ordering within parts as given in Table 3, leads to a different failure pattern:

$$\{15, 4, 9\} \cup \{10, 20, 7\} \cup \{15, 8\} \Rightarrow \{15, 10, 15; 20, 4, 8, 9, \{7\}\}$$

Failure time		Partition			Lives of standbys in the partitions	Sequence Buildup
Cum	Stage	I	II	III		
0	0	15, 10, 15			{4, 9}U{20, 7}U{8}	*
10	10	5, 20*, 5			{4, 9} U{7} U{8}	20
15	5	4*, 15, 0			{9} U{7} U{8}	20, 4
15	0	4, 15, 8*			{9} U{7} U{*}	20, 4, 8
19	4	9*, 11, 4			{*} U{7} U{*}	20, 4, 8, 9
23	4	5, 7, 0			{*} U{7} U{*}	20, 7, 8, 9, {7}

TABLE 3: Permutation of parts

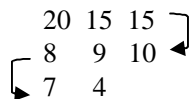
However, it should be noted that this particular permutation as shown in Table 3 leads to the situation at the final stage, where one of the 'parts' is exhausted, there are items in other parts (namely, when part III is exhausted, there is an item in part II with life 7 units), which are not yet introduced into the failure pattern table. In other words, in this example we have part III with only two elements, namely, {15, 8} has all its elements failed by 23 units; then, part I also has no spare element left, but part II has an element (of life 7 units) yet untouched as a spare. Hence, it is obvious that by transferring this element from part II to part III one can infuse another 5 (=min. {5, 7, 7}) units of life to the system. Of course, this gives rise to (or rather, changes the present partition into) the partition {15, 4, 9} U {10, 20} U {15, 8, 7} with the minimum $28 = 23 + \min.\{5, 7, 7\}$.

It is obvious that with a total $T_0 = 88$, with a part sum $S_{02} = 30$, an upper bound to the objective function is $\min\left(30, \left\lfloor \frac{88-30}{2} \right\rfloor\right) = 29$. By inspection of the present partition with $S_{0i} = 28, 30, 30$ one can see a further, final improved partition {15, 4, 10} U {9, 20} U {7, 8, 15} leading to the best value 29.

In this particular problem, it was possible to obtain- with a little inspection and intelligent guess-work, a solution value which equaled an upper bound to the optimal solution of the problem and hence one could get a solution which could be shown to be optimal and the obtained trial solution could be recognized as optimal; which need not be the situation in general. Hence a natural question arises: is there a computationally efficient way of picking up and recognizing an optimal solution? We shall present below a procedure which appears to achieve this aim.

Without loss of generality, we shall arrange the items in a non ascending order of their values and require that the partitions $S_{01}, S_{02}, \dots, S_{0k}$ are so named - or, as the algorithm proceeds, are rearranged (re-named) if necessary, such that $T_{01} \geq T_{02} \geq \dots \geq T_{0k}$. Thus the value of the partition will be also equal to T_{0k} .

We shall illustrate the algorithm by 'working out' an example problem. Consider the same example in section 2.1. Initially we arrange the elements as {20, 15, 15, 10, 9, 8, 7, 4} and form the $k = 3$ subsets as per the zigzag heuristic scheme as shown below:



It is leading to the parts $\{20, 8, 7\} \cup \{15, 9, 4\} \cup \{15, 10\}$, giving the part sums 35, 28, 25 while the 'ideal' upper bound is 29. Thus, the three part sums are having an excess of +6, -1, -4 from the bound and maximum of differences between part-sums is $35-25=10$. Since the part I, which is the biggest, has one element of value 7, less than 10, a simple transfer from part I to part III of this value 7 gives a better partition. But a transfer of value 7 from I to III leaves a 'deficit' of 1 in I, retaining its criticality, leading to $\{20, 8\} \cup \{15, 9, 4\} \cup \{15, 10, 7\}$ with part sums 28, 28, 32 with excess -1, -1, +3 and the solution value 28. Now the one part with positive excess, namely, III does not have an element of value not more than the maximum of differences between part sums (i.e., 4) and hence, no simple transfer of items can give a better partition. Any improvement, if at all possible, could be brought about only by an exchange - and not by simple transfer of elements between parts. Since 28 is an achieved value, we can see that no optimal partition can have part sums greater than $88-(28)2=32$. If it were possible to have an improved solution, of value 29, the largest allowable part sum will be $88 - 2(29) = 30$ only. Hence, one can now go for an implicit enumeration approach like the lexisearch, for picking up and establishing optimality of a partition.

As already noted, the partitions are made almost unique by defining only non-decreasing part-sums as valid. Further, the largest part sum, as just established, has to be between 30 and 29, if an optimal value of 29 can be obtained. In fact, with 29 as optimal value (the total of all parts being necessarily 88); the largest part sum should be 30 only in the present illustration. We now use the lexisearch algorithm to obtain optimal solution to the problem.

3. A LEXISEARCH ALGORITHM

The lexisearch algorithm is a systematic branch and bound approach, which derives its name from lexicography, the science of effective storage and retrieval of information. It was developed by Pandit [9], and since then it has been applied to many combinatorial optimization problems efficiently [2, 3].

In lexisearch algorithm, we first arrange the set of solutions of a problem in a hierarchy, like words in a dictionary, such that each incomplete word represents the block of words with this incomplete word as the leader of the block. We calculate bounds for the values of the objective function over these blocks of words. These bounds are then compared with the best solution value found so far. If no word in the block can be better than the best solution value found so far, then we jump over the block to the next one. However, if the bound indicates a possibility of better solutions in the block, we enter into the sub block by concatenating the present leader with appropriate letter and set a bound for the new (sub) block so obtained [2, 3, 9].

3.1. The algorithm

A pseudo-code for the lexisearch algorithm for our problem is as follows:

```

READ  $n, k$  and the component lives  $C_i$ , for  $i = 1, 2, 3, \dots, n$ ;
Set  $V_i = 0$ , for  $i = 1, 2, 3, \dots, n$ ;
Set  $X_{ij} = 0$ , for  $i = 1, 2, 3, \dots, k$ , and  $j = 1, 2, 3, \dots, (n-k+1)$ ;
Compute bound;
    
```

```

For i = 1 to (k-1) do
  Set j = m = sum = index(i) = Si = 0;
  Label - j:
  j = j + 1;
  if(j > n) then do the following:
    Si = Si - Cindex(i);
    j = index(i);
    index(i) = 0;
    Vi = 0;
    Xij = 0;
    m = m - 1;
    if(m < 0) then "Optimal solution is not possible", so, Stop.
      else go to Label - j;
    endif;
    if(Vi = 1) then
      go to Label - j;
    endif;
    sum = Si + Ci;
    if(sum > bound) then
      go to Label - j;
    endif;
    Si = sum;
    m = m + 1;
    Xij = Ci;
    index(i) = j;
    Vi = 1;
    If(Si = bound) then
      go to Label - k;
    endif;
    go to Label - j;
  Label - k:
endifor;
Set Sk = m = 0;
For j = 1 to n do
  if(Vj = 0) then
    Sk = Sk + Cj;
    m = m + 1;
    Xij = Cj;
  endif;
endifor;
Find Solution = min.{Si, i = 1, 2, 3, ....., k};
Print the Solution and Stop.

```

3.2. Illustration

The 'Search Table' for the life values {20, 15, 15, 10, 9, 8, 7, 4} is shown in Table 4. Thus an optimal partition is {20, 9} U {15, 10, 4} U {15, 8, 7}. This optimal partition with sequence and failure pattern is shown in Table 5. So, the optimal sequence is {20, 15, 15; 10, 8, 9, 7, 4}.

20 ₍₂₀₎ , 15 ₍₃₅₎ *	
15 ₍₃₅₎ *	
10 ₍₃₀₎ *	
9 ₍₂₉₎ ; [15,15,10,8,7,4]	
15 ₍₁₅₎ 15 ₍₃₀₎ *	
10 ₍₂₅₎ , 8 ₍₃₃₎ *	
7 ₍₃₂₎ *	
4 ₍₂₉₎ ; [15,8,7]	
15 ₍₁₅₎ , 8 ₍₂₃₎ , 7 ₍₃₀₎	

TABLE 4: Search Table.

Failure time		Partition			Lives of standbys	Sequence
Cum	Stage	I	II	III	in the partitions	Buildup
0	0	20, 15, 15			{9} U {10,4} U {8,7}	*
15	15	5, 10*, 8*			{9} U {4} U {7}	10,8
20	5	9*, 5, 3			{*} U {4} U {7}	10,8,9
23	3	6, 2, 7*			{*} U {4} U {*}	10,8,9,7
25	2	4, 4*, 5			{*} U {*}	10,8,9,7,4
29	4	*, *, 1				

TABLE 5: Optimal partition with failure pattern

4. A GENETIC ALGORITHM

Genetic Algorithms (GAs) are computerized search and optimization algorithms based on the mechanics of natural genetics and natural selection [1, 7]. They are robust search algorithms which are suited for problems having comparatively larger solution spaces. However, they are essentially heuristic and, by themselves, can not guarantee the optimality of the solutions they produce.

They start from a population of chromosomes and then apply three operators: reproduction/ selection, crossover and mutation to create new, and hopefully better populations. The operator 'crossover' together with the operator 'reproduction' is the most powerful process in the GA search. The frequency of mutation is usually chosen to be considerably less than the frequency of crossover.

4.1. Genetic modeling of the problem

As a first step in applying the GA to the present problem, the solution space is to be mapped into the chromosomes of length n, the number of elements to be partitioned. In a chromosome, the genes indicate to which 'part' a particular element should belong. Then, for k-part problem of length n, one has to have k genes - e.g., 1, 2, ..., k representing k-parts. The chromosome structure will then indicate the partition. For instance, let k=3 and n=8. Then, the chromosomes will be of length 8 with three genes, say, 1, 2 and 3. So, a chromosome will be the set of all ternary strings of length eight. The chromosome (3, 3, 2, 2, 1, 2, 1, 2) stands for the partition $P_1 = \{C_5, C_7\}$, $P_2 = \{C_3, C_4, C_6, C_8\}$, and $P_3 = \{C_1, C_2\}$, where C_1, C_2, \dots, C_8 are the component lives arranged in non-increasing order. For any partition, the value of objective function is defined as the minimum of the part-sums. The fitness of the solution is decided by this objective function which has to be maximized. For a set of 8 components with lives {20, 15, 15, 10, 9, 8, 7, 4} arranged in non-ascending order, one of the chromosomes may be (1, 2, 3, 1, 2, 3, 1, 2) representing the partition {20, 10, 7} U {15, 9, 4} U {15, 8} with objective function value 23 = min {37, 28, 23}.

4.2. Genetic operators

There are many variations of GAs formed by using different reproduction, crossover and mutation operators. In our implementations, stochastic remainder selection method [6], the multi-point crossover operator [7] that interchanges the alternative sub-strings at randomly selected points, and the swap mutation operator [1] which selects any two genes randomly and exchanges them, have been considered.

The GA approach has been claimed to lead to very good, near-optimal solutions. However, the approach is obviously 'controlled or guided' by choice of parameters: namely, probability of crossover (P_c), probability of mutation (P_m), population size (P_s), and of course crossover points and mutation locations. As Deb [6] points out: successful working of GAs depends on a proper selection of these parameters, but often one is in the dark as to what values should be taken for these parameters. For our problem, several runs were executed with different settings of the parameters for different value

of n and k . These runs allowed us to fine-tune the parameters. After substantial testing, we settled the parameters as: $P_c=0.9$, $P_m=0.1$ and $P_s=100$.

5. COMPUTATIONAL EXPERIENCE

The lexisearch algorithm (LSA) and genetic algorithm (GA) have been coded in Visual C++ on a Pentium 4 personal computer with speed 3 GHz and 448 MB RAM under MS Windows XP, and tested some randomly generated problems of different sizes drawn uniformly from various ranges of data with different values of n and k . Each system contains 20 problem instances. We include two statistics to summarize the results by the algorithms: average and standard deviation of solution time and solution ratios (only for GA). Solution ratio is defined as ratio of best solution value obtained by GA to the exact solution value obtained by LSA. Tables 6 and 7 summarize the results by the algorithms for the randomly generated instances drawn from the interval $[1, 100]$ and $[1, 10000]$ respectively.

N	K	LSA		GA			
		Time		Sol. Ratio		Time	
		Mean	Std Dev	Mean	Std Dev	Mean	Std Dev
100	10	0.01	0.02	1.00	0.02	0.11	0.03
	20	0.03	0.05	1.00	0.05	0.15	0.05
200	20	0.13	0.07	1.00	0.03	0.22	0.09
	30	0.16	0.13	1.01	0.09	0.27	0.12
300	30	0.75	0.25	1.00	0.08	0.80	0.21
	40	0.92	0.35	1.01	0.12	0.79	0.20
400	40	2.24	1.03	1.01	0.15	2.18	0.84
	50	2.57	1.54	1.00	0.07	2.27	1.03
500	50	4.59	1.87	1.01	0.23	3.37	1.32
	60	5.64	2.43	1.02	0.56	4.77	1.55

TABLE 6: Results by the algorithms for the instances drawn from the interval $[1, 100]$.

N	K	LSA		GA			
		Time		Sol. Ratio		Time	
		Mean	Std Dev	Mean	Std Dev	Mean	Std Dev
100	10	0.02	0.02	1.00	0.02	0.12	0.03
	20	0.03	0.03	1.00	0.02	0.15	0.05
200	20	0.14	0.08	1.01	0.05	0.23	0.07
	30	0.19	0.18	1.01	0.12	0.26	0.11
300	30	0.73	0.21	1.00	0.07	0.81	0.21
	40	0.98	0.37	1.00	0.15	0.78	0.22
400	40	2.57	0.92	1.01	0.12	2.15	0.85
	50	2.89	1.05	1.01	0.09	2.28	1.01
500	50	5.09	2.07	1.02	0.20	3.34	1.29
	60	5.78	2.73	1.02	0.65	4.76	1.51

TABLE 7: Results by the algorithms for the instances drawn from the interval $[1, 10000]$.

It is clear from the Tables 7 and 8 that for $n < 300$, GA takes more time than LSA, but as size increases LSA takes more time than GA. Of course, as the size increases solution quality by GA

decreases. Also, it is seen that for same n when k increases the solution quality by GA decreases. For a value of n , computational times do not vary much for the different values of k for both algorithms.

6. DISCUSSIONS AND CONCLUSIONS

The deterministic replacement problem for serial system is viewed in such a way that lexisearch and genetic algorithms can be applied. Computational experience shows that both the algorithms are suitable for the problem. However, for the small sized instance, lexisearch algorithm is found to be better one. In order to investigate the robustness of GAs, for each size, 20 instances were solved. Though the solution quality is good by GA for smaller sized instances, but the computational time is higher than that of by lexisearch algorithm. It is to be noted that for some systems the exact optimal solutions were not possible. As a whole, GA is good. The success of GA for the problem suggests the use of this technique in many other industrial fields, particularly in maintenance and reliability. Again the successful working of GA depends on the proper selection of GA parameters. So, carefully choosing the parameters may lead to a better performance of genetic algorithms on the above problem. We did not consider any case study for this problem, which may be considered, in future, to show the effectiveness of the algorithms. Also, we did not consider service cost/time, which may be considered in future.

Acknowledgements

The author wishes to acknowledge Prof. S. N. Narahari Pandit, Centre for Quantitative Methods, Osmania University, Hyderabad, India, for his valuable suggestions and moral support. The author is also thankful to the honorable anonymous reviewer for his comments and suggestions.

7. REFERENCES

- [1] Z.H. Ahmed. "Genetic algorithm for the traveling salesman problem using sequential constructive crossover". International Journal of Biometrics & Bioinformatics 3, pp. 96-105, 2010.
- [2] Z.H. Ahmed. "A lexisearch algorithm for the bottleneck traveling salesman problem". International Journal of Computer Science and Security 3, pp. 569-577, 2010.
- [3] Z.H. Ahmed. "A sequential constructive sampling and related approaches to combinatorial optimization". PhD Thesis, Tezpur University, Assam, India, 2000.
- [4] Z.H. Ahmed, S.N.N. Pandit, and M. Borah. "On the solution of a deterministic replacement problem". Presented in National Seminar on Advancing Frontiers in Statistics and Operations Research, Dibrugarh University, Assam, India, During September 22 - 24, 1997.
- [5] L. Cui and H. Li. "Opportunistic maintenance for multi-component shock models". Journal of Mathematical Methods of Operations Research 63(3), pp. 180-191, 2006
- [6] K. Deb. "Optimization for engineering design: algorithms and examples". Prentice Hall of India Pvt. Ltd., New Delhi, India, 1995.
- [7] D.E. Goldberg. "Genetic algorithms in search, optimization, and machine learning". Addison Wesley, Reading, MA, 1989.
- [8] J.D.E. Little, K.G. Murthy, D.W. Sweeny and C. Karel. "An algorithm for the travelling salesman problem". Operations Research 11, pp. 972-989, 1963.
- [9] S.N.N. Pandit. "Some quantitative combinatorial search problems". PhD Thesis, Indian Institute of Technology, Kharagpur, India, 1963.

- [10] K.S. Park. "*Reliability of a system with standbys and spares*". Journal of Korean Institute of Industrial Engineering 3(1), Dec 1977.
- [11] L.M. Pintelon and L.F. Gelders. "*Maintenance management decision making*". European Journal of Operational Research 58(3), pp. 209-218, 1985.
- [12] M.S. Samhouri, A. Al-Ghandoor, R.H. Fouad and S.M.A. Ali. "*An intelligent opportunistic maintenance (OM) system: a genetic algorithm approach*". Jordan Journal of Mechanical and Industrial Engineering 3(4), pp. 246-251, 2009.
- [13] A. Savic, G. Walters and J. Knezevic. "*Optimal, opportunistic maintenance policy using genetic algorithms, 2: analysis*". Journal of Quality in Maintenance Engineering 1(3), pp. 25-34, 1995.
- [14] K.-H. Wang and B.D. Sivazlian. "*Life cycle cost analysis for availability and reliability of series system with warm standbys components*". International Conference on Computers and Industrial Engineering, Puerto Rico, U.S.A., 1997.
- [15] H. Wang. "*A survey of maintenance policies of deteriorating systems*". European Journal of Operational Research 139, pp. 469-489, 2002.
- [16] H. Wang and H. Pham. "*Reliability and Optimal Maintenance*". Springer, 2006.
- [17] X. Zhaou, L. Xi and J. Lee. "*A dynamic opportunistic maintenance policy for continuously monitored system*". Trans. J. of Quality Management Engineering 12(3), pp. 294-305, 2006.
- [18] X. Zhaou, L. Xi and J. Lee. "*Opportunistic preventive maintenance scheduling for a multi-unit series system based on dynamic programming*". International Journal of Production Economics, 2008.

Optimal Sensing for Opportunistic Spectrum Access in Cognitive Radio

Nasrullah Armi

*Electrical and Electronics Department
PETRONAS University of Technology
Bandar Seri Iskandar, Perak, 31750, Malaysia*

armi@ppet.lipi.go.id

Naufal M. Saad

*Electrical and Electronics Department
PETRONAS University of Technology
Bandar Seri Iskandar, Perak, 31750, Malaysia*

naufal_saad@petronas.com.my

M. Zuki Yusoff

*Electrical and Electronics Department
PETRONAS University of Technology
Bandar Seri Iskandar, Perak, 31750, Malaysia*

mzuki_yusoff@petronas.com.my

Muhammad Arshad

*Electrical and Electronics Department
PETRONAS University of Technology
Bandar Seri Iskandar, Perak, 31750, Malaysia*

muhammadarshad@comsats.edu.pk

Abstract

One of the most difficult thing but important problem when designing an OSA (Opportunistic Spectrum Access) MAC protocol is how the unlicensed users decide when and which channel they should sense and access without conflicting the communications among PUs. To solve this problem, the unlicensed users should have the ability of adaptively and dynamically seeking and exploiting opportunities in both licensed and unlicensed spectrum and along both of the time and the frequency dimensions. Secondary Users (SUs) as unlicensed users are required to sense radio frequency band, and when PU are detected, they must vacate the channel immediately within certain amount of time. Due to hardware and energy constraints, full spectrum availability cannot be sensed as well as they do not monitor when there is no data to be transmitted. In this paper, we study MAC protocol design and optimal sensing for OSA in Cognitive Radio (CR) ad hoc network under Partially Observable Markov Decision Process (POMDP) algorithm that maximizes achievable throughput for SUs with sufficient protection to PUs. The bandwidth effect to number of bit transmitted in one slot and tractable greedy algorithm to reduce the complexity of POMDP calculation was studied as well. The derivation of greedy approach proves that sensing problem can be solved either optimally or approximate the optimal solution. Computer simulation is used to evaluate the performances both of optimal and sub optimal strategy.

Keywords: Dynamic Spectrum Access, Opportunistic Spectrum Access, POMDP, Greedy Algorithm, Cognitive Radio

1. INTRODUCTION

Dynamic Spectrum Access (DSA) systems are one of the most promising technologies available to increase the range and efficiency of spectrum dependent services [1]. DSA systems locate unused spectrum, and organize their users to operate within the spectrum they have identified. DSA systems ensure that no interferences to other users by scanning and sensing the spectrum environment, as the Defense Advanced Research Projects Agency NeXt Generation (DARPA XG) spectrum sharing field tests have established, or through pre-existing knowledge, such as the geolocation database proposed for unlicensed access to TV band white space, or a combination of both.[2]. Shortly, DSA affords the benefits to spectrum allocation problems such as providing the increased density, better system management, and inherent in-channel and co-site interference resolution as well as it enables opportunistic access to the spectrum for uncoordinated sharing of spectrum on a non-interference basis. In addition, the other projects related to DSA and CR networks that have been developed are DIMSUMnet project [3], DRiVE/overdrive project [4], E2R and E3 [5]. These projects aim to resolve the current inefficient usage of spectrum band and make the radio has the ability to intelligently recognize the status of radio spectrum environment and adaptively change its transmission parameter such as transmission frequency and bandwidth, power efficiency, and modulation scheme, etc.

According to the hierarchical access model, licensed spectrum is opened to SUs under the condition that it does not interfere with PUs beyond a certain probability of collision [6][7]. Spectrum underlay and overlay are two strategies allowing the coexistence of primary and secondary users. Underlay refers to the approach where the transmission power of SUs is limited to be less than the noise floor of PUs, whereas overlay does not limit the transmit power of SUs but imposes restriction on when and where SUs can transmit [8]. The hierarchical access model is likely the most compatible with the current spectrum management policies and provides better spectrum efficiency in the licensed bands.

OSA itself is referred to as DSA, and often included as part of the larger concept of cognitive radios. It has emerged as a way to dramatically improve spectrum utilization. The basic idea is to allow SUs to identify available spectrum and characterize the presence of PUs. According to that information, the unlicensed devices identify communication opportunities (spectrum holes) in frequency, time, or even code, and transmit using those opportunities in a manner that limits the interference perceived by PUs. Furthermore, the design of OSA MAC protocols imposes new challenges that are not considered in the conventional wireless networks. One of the most difficult but important problem in designing an OSA MAC protocol is how the unlicensed users decide when and which channel they should sense and access without conflicting the communication to PUs.

According to the network architecture, CR networks can be classified into the infrastructure based and ad hoc networks [9]. The infrastructure-based CR network has a central coordinator such as base station in cellular network or an access point in WLANs. The observations performed by each CR user feed to the CR base station and CR base station decides which channel CR user can access. Then, CR user reconfigures its communication parameter, i.e. power, type of modulation, etc. On the other hand, CR ad hoc network does not have any infrastructure backbone. Hence, CR users communicate with others through the ad hoc connection on both licensed and unlicensed spectrum bands.

CR MAC protocol has responsibilities to coordinate channel access to licensed bands. It enables multiple CR users to share the spectrum resource by determining who will access the channel and when it will be performed. This protocol design is necessary to accomplish the Quality of Service (QoS) of data transmission. In [10], CR MAC protocol for ad hoc network is classified into

three classes, which are random access, time slotted, and hybrid protocol. Random access protocol does not need time synchronization, and generally based on Carrier Sense Multiple Access Collision Avoidance (CSMA/CA) principle. CR user monitors the spectrum bands to detect whether there is transmission from the other CR users. Data packet is transmitted after back off duration. Time slotted protocol need network wide synchronization, where time is divided into slots for both the control channel and the data transmission. Meanwhile, hybrid protocol is combination of random access and time slotted protocol. This protocol uses a partially slotted transmission, in which the control signaling generally occurs over synchronized time slots and random channel access for data transmission. POMDP frameworks for CR was proposed in [11] as one of hybrid protocol model for CR MAC, where limited sensing capabilities of CR imply that only part of channel can be sensed at one time. The adopted approach integrates the design of spectrum access protocol at the MAC layer with spectrum sensing at the physical layer and traffic statistics determined by the application layer. A similar approach is used in the CR access scheme in [12].

Most of the previous works on the throughput of CR user focus on the fundamental tradeoff between sensing capability and achievable throughput. In [13] throughput of SU relating to sensing time in local and cooperative spectrum sensing was investigated under two distinct scenarios, Constant Primary User Protection (CPUP) and Constant Secondary User Spectrum Usability (CSUSU). Furthermore, the throughput enhancement by implementing cooperative sensing strategy was proposed in [14]. The presented simulation results show that the effectiveness of the proposed sensing strategy improves the throughput of CR users and decreases the interference to the PUs. The design of sensing slot duration to maximize the achievable throughput of SUs under the constraint that PU is sufficiently protected was studied in [15]. Using energy detector, the author presented the trade off between sensing time and achievable throughput of SU.

In this paper, we study optimal sensing strategy that maximizes bit transmitted of SUs based on POMDP model and under the constraint that PU is sufficiently protected. We focus on study of cognitive MAC protocol design for OSA where each SU must sense the channel intelligently by statistical traffic behavior and decide to transmit the data based on the sensing outcome. The rest of the paper is organized as follows. In section II, we give description of policy strategy for optimal and sub optimal in channel sensing and access. The detail system model is described in section III. The numerical results and discussion are presented along with some comparisons in section IV. Finally, conclusion and future works are presented in the following section.

2. POLICY STRATEGY

Decision-making is the cognitive process leading to the selection of action among variations. One-way to automate the decision making process is to provide a model of dynamics for the domain in which the machine will be making decisions. A reward structure can be used to motivate immediate decision that will maximize the future reward.

POMDP is an aid in the automated decision-making. POMDP policy informs CR users what action to be executed. It can be a function or a mapping and typically depends upon the channel states. In this section, we provide detail formulation of policy strategy either optimal and sub optimal based on greedy approach for sensing decision.

2.1 Optimal Strategy

Channel access based on POMDP is known as an optimal strategy which model the channel opportunity of network system as discrete time Markov chain with number of channel state and formulate as $M=2^N$ states, where N is number of channel. The state diagram for N=2 is described

in figure 1 where $\bar{\alpha}_i = 1 - \alpha_i$ and state (0,1) indicates the first channel is available and the second channel is busy. The term of partially observable mean that CR user selects set of channels to be sensed and set of channels to be accessed based on sensing outcome. This

objective is to maximize the throughput of SUs under the constraint of interference to PU by exploiting the sensing history and the spectrum occupancy statistics.

The design of OSA protocol that maximizes the throughput of SU can be formulated as POMDP over finite horizon. It is defined by tuple $\{S,A,P,\Theta,R\}$, where S denotes a finite set of states with state i denoted by s_i , A denotes a finite set of actions with action i denoted by a_i , P denotes the transition probabilities $P_{i,j}$ for each action in each state as function of $\{\alpha_i, \beta_i\}_{i=1}^N$ which describes the channel availability of PU networks, R denotes the reward structure (r_{j,A_1,A_2}) which is defined as number of transmitted bits in one slot when CR user take an action, and Θ is observation where SUs observe the availability of channel at state j , $\Theta_{j,A_1} \in \{0,1\}^{|A_1|}$. The reward is proportional to its bandwidth and formulated as follows:

$$r_{j,A_1,A_2}(t) = \sum_{i \in A_2} S_i(t) B_i \tag{1}$$

Figure 2 shows Markov dynamics process model where observations are made after an action is taken. Equivalently, observation could have been taken before actions.

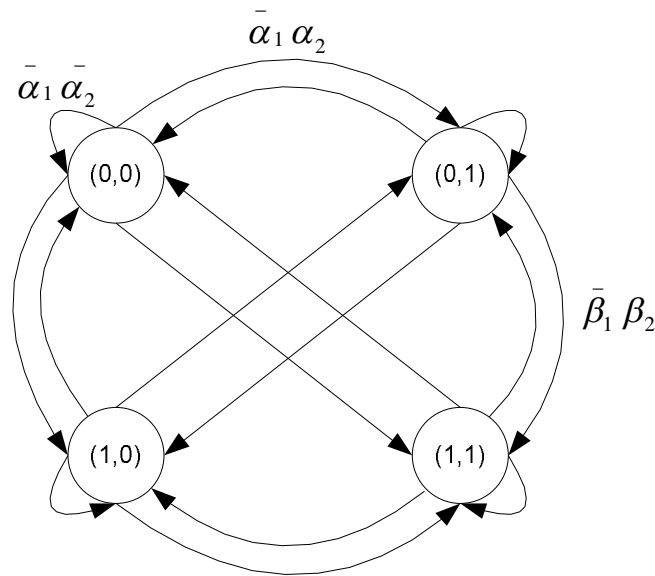


FIGURE 1: State diagram for N=2 as Markov process model

In POMDP model, the system state is not directly known, however CR users can observe to learn the most likely state. The observation yields the current system state. Then, the information state, also known as belief vector $\pi = (\pi_1, \dots, \pi_M)$, aids in determining the most likely state of primary network by storing all previous actions and observations in a summary statistic. The belief vector is probability distribution over state of the channels.

Belief vector π is a sufficient statistic for the optimal policy and behaves as a discrete time continuous state Markov process. The users observe with distribution probability under system channel states. The information state is updated after each action and observation with the application of Bayes' rule as follows:

$$\pi'_j = \frac{\sum_{i=1}^M \pi_i p_{i,j} \Pr[\Theta_{j,a} = \theta]}{\sum_{i=1}^M \sum_{j=1}^M \pi_i p_{i,j} \Pr[\Theta_{j,a} = \theta]} \tag{2}$$

The resulting information state is vector of probabilities computed using the above formula and the information transformation function is given by

$$\pi' \cong [\pi'_1, \dots, \pi'_M] \cong \tau(\pi|a, \theta) \tag{3}$$

In POMDP model, the policy maps the information states into action and maximizes the expected total reward. There are an infinite number of information states, since it is probability distribution over all states and stores the policy or value function in the form of tables. The maximum value function for all actions is given by the following formula:

$$V_t(\pi) = \max_{a=1, \dots, N} \left\{ \sum_{i=1}^M \pi_i \sum_{j=1}^M p_{i,j} \sum_{\theta=0}^1 \Pr[\Theta_{j,a} = \theta] (\theta B_a + V_{t+1}(\tau(\pi|a, \theta))) \right\} \tag{4}$$

Where $V_t(\pi)$ denotes the maximum expected reward that can be accrued in the remaining t decision intervals when the current information vector is π .

It is shown in [16] that $V_t(\pi)$ is piecewise linier and convex (PWLC) and can be written simply as

$$V_t(\pi) = \max_k \pi \gamma_k(t) \tag{5}$$

For some set of M dimensional column vectors $\{\gamma_k(t)\}$. The set of γ -vectors represents one of linier pieces coefficient for piecewise linier function. These piecewise linier functions can represent the value functions for each step in the finite horizon POMDP problem. The value function drawn over the information state is shown in fig.3

2.2 Sub Optimal Strategy based on Greedy Approach

Due to the complexity of optimal policy computation when number of slot and channel increase, Q.Zhao et al in [11] proposes sub optimal protocol based on a greedy approach. They reduced the dimension of states from exponential to linear by regarding to N , i.e. from $M=2^N$ to N state. The recursive equation to maximize the expected reward is formulated as follows:

$$\begin{aligned} W_t(\Omega) &= (\omega_{a_*} \beta_{a_*} + (1 - \omega_{a_*}) \alpha_{a_*}) B_{a_*} + \sum_{\theta=0}^1 \Pr[\Theta_{a_*} = \theta | \Omega, a_*] W_{t+1}(\tau(\Omega|a_*, \theta)) \\ &= (\omega_{a_*} \beta_{a_*} + (1 - \omega_{a_*}) \alpha_{a_*}) B_{a_*} + [\omega_{a_*} (1 - \beta_{a_*}) + (1 - \omega_{a_*}) (1 - \alpha_{a_*})] W_{t+1}(\tau(\Omega|a_*, 0)) + \\ &\quad [\omega_{a_*} \beta_{a_*} + (1 - \omega_{a_*}) \alpha_{a_*}] W_{t+1}(\tau(\Omega|a_*, 1)) \end{aligned} \tag{6}$$

where $W_t(\Omega)$ denotes the expected remaining reward starting from slot t achieved by greedy approach, $\tau(\Omega|a_*, \theta)$ denotes the updated information on channel availability given the

observation θ under action a , and $(\omega_{a_*} \beta_{a_*} + (1 - \omega_{a_*}) \alpha_{a_*})$ denotes the probability of availability for channel a in slot t . The notation of a_* is the chosen action in slot t to maximize the expected immediate reward and given by

$$a_*(t) = \arg \max_{a=1, \dots, N} (\omega_a(t) \beta_a + (1 - \omega_a(t)) \alpha_a) B_a \tag{7}$$

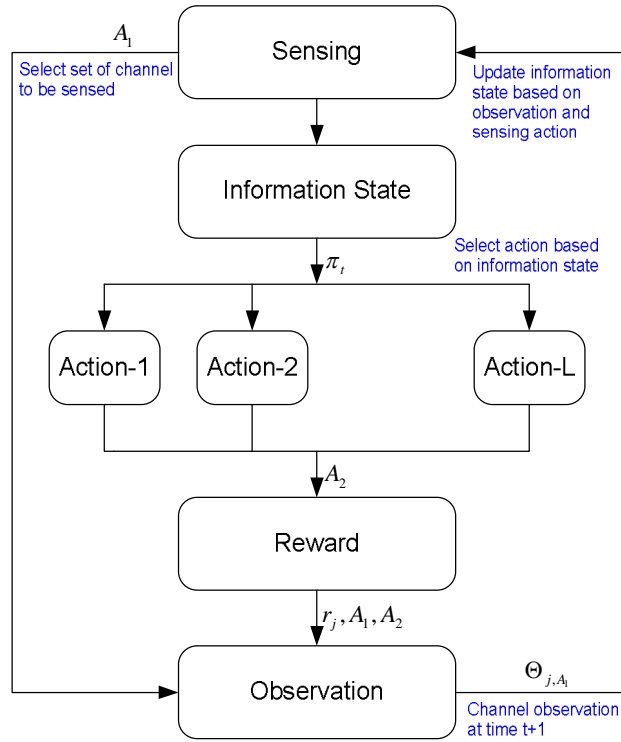


FIGURE 2: POMDP dynamic model

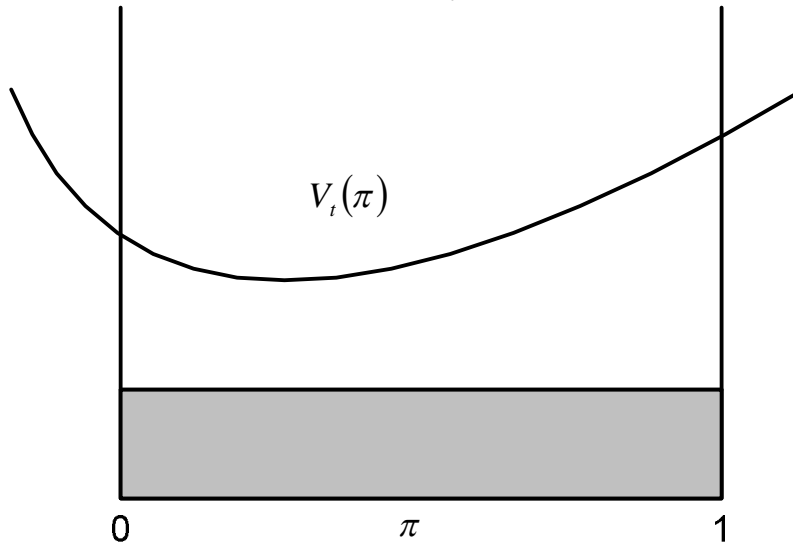


FIGURE 3: Value function drawn over information space

3. SYSTEM MODEL

The spectrum contains number of channel is licensed to PUs and have an authority to use it. However, when channel is not used, SUs can access the channel with prior to observe whether channel is available to avoid interference to PUs. We consider group of SUs sense and monitor primary channels which change depends on the time step and switch from occupied and unoccupied according to Markov chain. The existed channels are shared among PUs and a large of number SUs.

There are number of channels considered in this study and state of these channels change independently. Each channel has the bandwidth B_i ($i=1, \dots, N$). The state diagram and a sample path of the state evolution for $N=3$ are illustrated in fig.4. The state of channel $S_n(T)=\{1,0\}$ indicates that channel is busy and idle. In the system, transmission time is divided into slots of equal length T , where slot k refers to the discrete time period $[kT, (k+1)T]$. The structure of the each slot is described in fig.5. At the beginning of each slot, SUs sense set of the channels (L_1). Based on the sensing outcome, SUs will decide which channel to be accessed (L_2), where $L_2 \leq L_1 \leq N$. At the end of the slot, SU will send the acknowledgement signal that indicates successful transmission. The traffic statistics of the primary network follows a discrete time Markov process with number of states. Furthermore, secondary network is seeking spectrum opportunity in these N channels. Ad hoc network is assumed in which SUs sense and access the spectrum channel independently without exchanging local information.

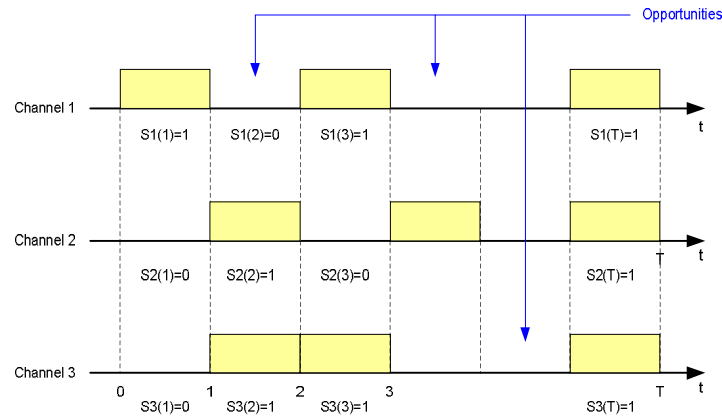


FIGURE 4: Spectrum occupancy for $N=3$

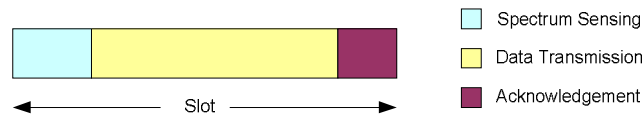


FIGURE 5: The slot structure

4. NUMERICAL RESULTS AND DISCUSSION

In this section, computer simulation results are presented to evaluate the performance of optimal and sub optimal based on the greedy approach with throughput metric as a function of slot number.

4.1 Optimal Cognitive MAC Protocol

This sub section presents the performance of optimal cognitive MAC based on POMDP model. We assumed that sensing errors is ignored in this simulation. Three channels are considered with the same bandwidth $B=1$ and number of slots (T) is 25. We have two cases with different transition probabilities (α, β). In case 1, probability of channel transition from idle (0) to busy (1) is 0.3, whereas channel remain unchanged from idle state is 0.7. Case 2 is the opposite of case 1, where the probability of channel remains unchanged ($\beta=0.3$) is lower than probability of channel transition ($\alpha=0.7$).

As shown in fig.6 that throughput of SU increases over time in both cases. Due to the probability of channel remains unchanged in case 1 greater than case 2, hence the throughput of SU in case 1 is higher than case 2. Higher probability of channel remain unchanged cause case 1 has more time of data transmission than case 2 without interruption by transition of channel state. In fig.7,

8, and 9, we set the value of channel bandwidth (B) to 5, 10, and 20 respectively, and then keep the other parameters constant. The result shows that by increasing the value of channel bandwidth cause number of transmitted bit of SU over channel increases significantly.

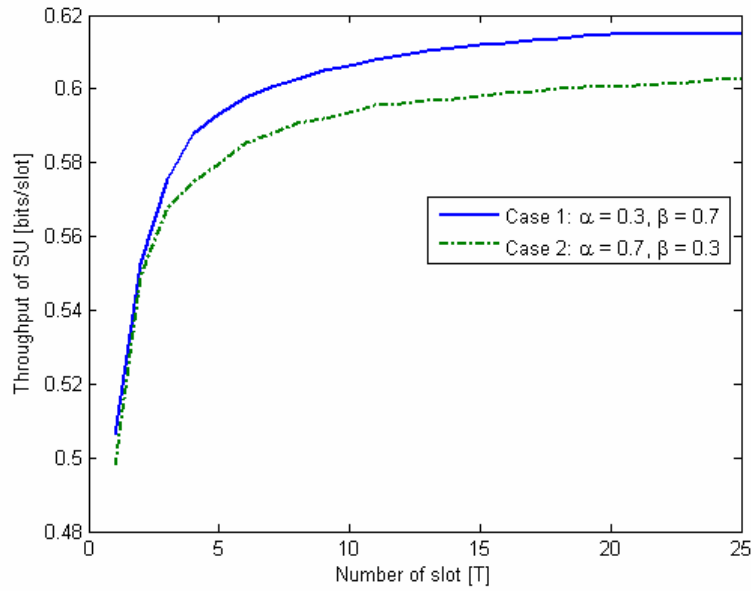


FIGURE 6: Achievable throughput of SU with parameter setup B=1, N=3, T=25

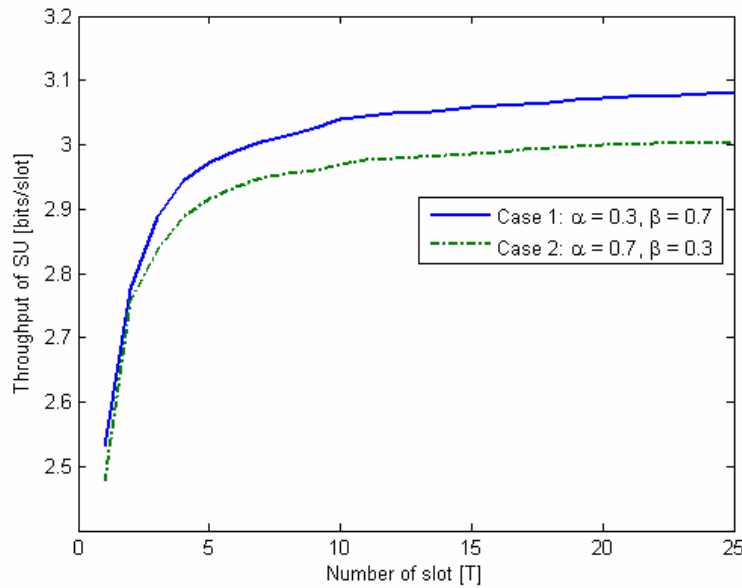


FIGURE 7: Achievable throughput of SU with parameter setup B=5, N=3, T=25

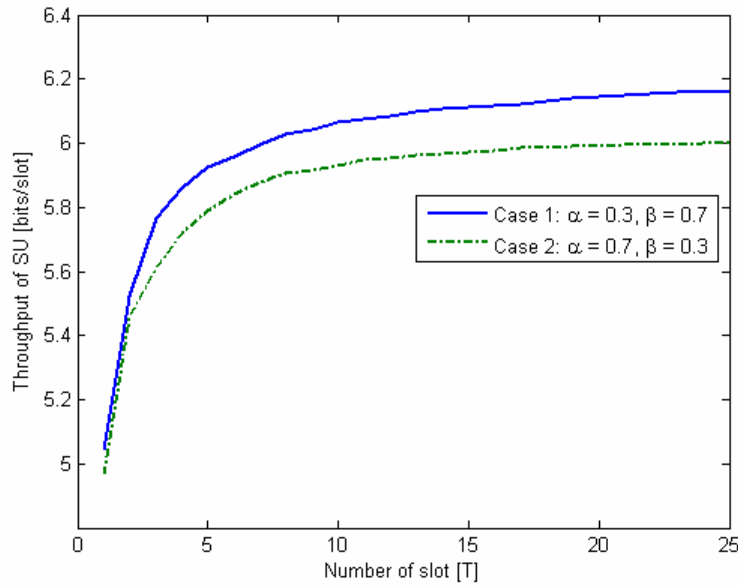


FIGURE 8: Achievable throughput of SU with parameter setup B=10, N=3, T=25

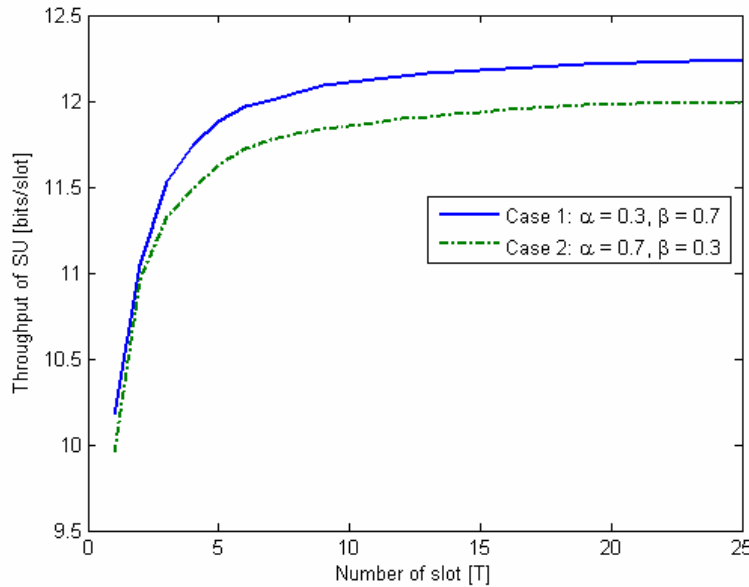


FIGURE 9: Achievable throughput of SU with parameter setup B=20, N=3, T=25

4.2 Sub-optimal Cognitive MAC Protocol

This sub section presents the performance of sub optimal strategy based on greedy approach as compared to the optimal strategy. The same as aforementioned parameters above that sensing error was ignored in this simulation. Three channels (N=3) is considered with the same bandwidth B=1, number of slots (T) is 25. Transition probabilities (α, β) were set to (0.2,0.8). According to fig.10, this simulation parameter setup yields the throughput of SU for greedy approach relatively match and nearly equal to optimal strategy. However, when setup is converted to multiple bandwidths B=[0.75,1,1.5] with different transition probabilities $\alpha_i=[0.8,0.6,0.4]$ and $\beta_i=[0.6,0.4,0.2]$ as described in fig.11, the greedy approach has the performance loss.

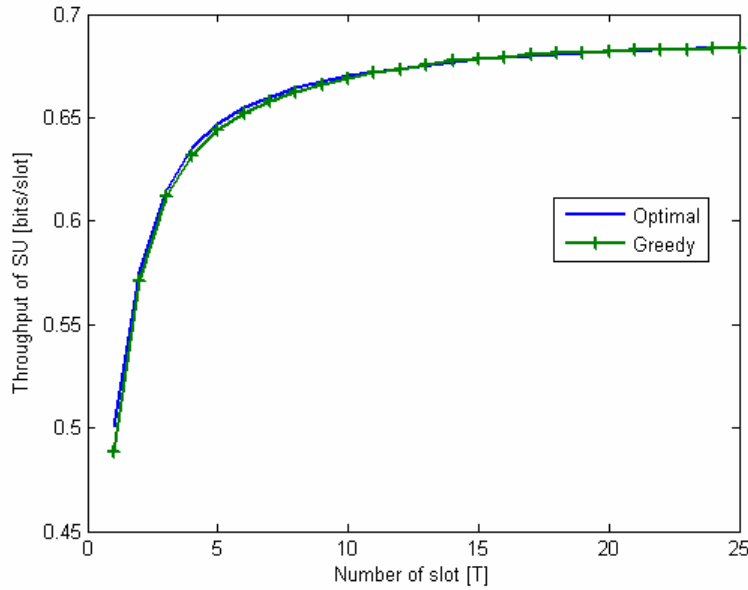


FIGURE 10: Performance comparison between optimal and greedy approach with parameter setup $B=1$, $N=3$, $T=25$, $\alpha=0.2$ and $\beta=0.8$

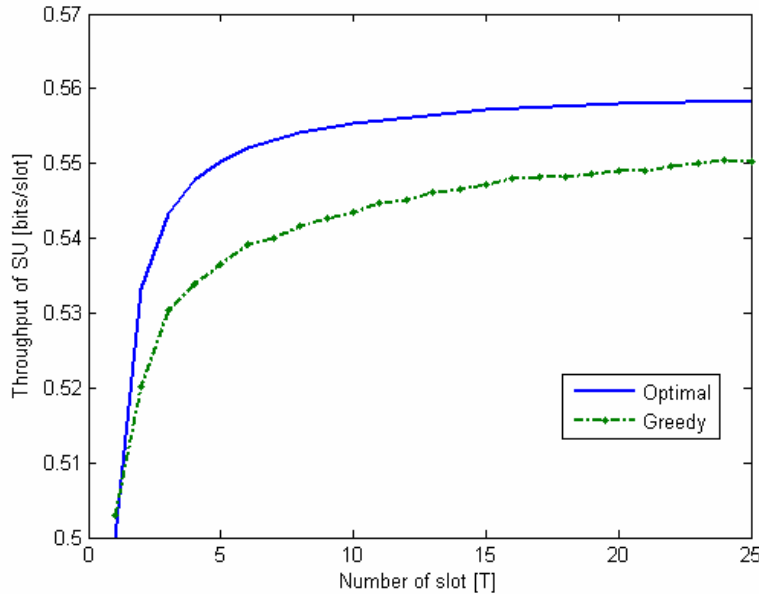


FIGURE 11: Performance comparison between optimal and greedy approach with multiple bandwidths $[0.75, 1, 1.5]$ and transition probabilities $\alpha_i=[0.8, 0.6, 0.4]$ and $\beta_i=[0.6, 0.4, 0.2]$

5. CONCLUSION AND FUTURE WORKS

The performance of OSA in CR ad hoc network by considering SUs interest was studied. POMDP model was implemented to evaluate the throughput as function of slot number. The results show that the optimal strategy maximizes the average number of bits transmitted by the SU in T slots. Furthermore, increasing channel bandwidth cause number of bit transmitted in one slot increase significantly. Due to the complexity of POMDP model when channel increases, greedy approach as a sub optimal strategy was studied. It yields the throughput of CR user match and nearly close to optimal strategy. However, sensing errors are ignored in this study. Hence, in the future works,

we will consider false detection and miss-detection in PU signal sensing. Then, cooperative signal detection technique will be implemented. Cooperative technique can improve probability of detection with less sensing errors where each CR users cooperatively sense primary channels. Furthermore, trade off between sensing action and throughput as well as kind of application such as multimedia application over CR networks will be further investigated.

6. REFERENCES

- [1] Q.Zhao, B.M.Sadler. "A Survey of Dynamic Spectrum Access". IEEE Signal Processing Mag, Vol.2. No.3, pp. 79-89, 2007.
- [2] "DARPA: The Next Generation (XG) Program". <http://www.darpa.mil/ato/programs/xg/index.htm>
- [3] M.Buddhikot, P.Kolodzy, S. Miller, K.Ryan and J.Evans. "DIMSUMnet: New Directions in Wireless Networking Using Coordinated Dynamic Spectrum Access". IEEE WoWMoM05, June 2005.
- [4] L.Xu, R.Tonjes, T.Paila, W.Hansmann, M.Fank and M.Albrecht. "DRiVE-ing to The Internet: Dynamic Radio for IP Services in Vehicular Environments". In Proc. 25th Annual Conf. on LCN, USA, 2000.
- [5] E3 Project <http://ict-e3.eu>
- [6] R.Etkin, A.Parekh, and D.Tse. "Spectrum Sharing for Unlicensed Bands". IEEE J.Sel. Areas Communication. Vol.25, No.3, pp.517-528, April 2007.
- [7] J.Huang, R.A.Berry, and M.L.Honig. "Spectrum Sharing with Distributed Interference Compensation". In Proc. IEEE Int. Symp. On New Frontiers in Dynamic Spectrum Access Networks, p.88-93 Nov.2005.
- [8] J.Mitola. "Cognitive Radio: An Integrated Agent Architecture for Software Defined Radio". PhD Dissertation, Royal Inst. Tech. (KTH), Stockholm, Sweden, 2000.
- [9] I.F. Akyildiz, W.Y. Lee, M.C. Vuran, M. Shantidev. "Next Generation/Dynamic Spectrum Access/Cognitive Radio Wireless Networks: a survey". Computer Network Journal (Elsevier), Vol.50, Issue 13, p.2127-2159, 2006.
- [10] I.F. Akyildiz, W.Y. Lee, K.R. Chowdury. "CRAHNS: Cognitive Radio Ad Hoc Networks". Journal of Ad Hoc Networks, p.810-836, ScienceDirect, 2009.
- [11] Q.Zhao, L.Tong, A.Swami, Y.Chen. "Decentralized Cognitive MAC for Opportunistic Spectrum Access in Ad Hoc Network: A POMDP Framework". IEEE J, Selected Areas Comm. Vol.25 No.3, p.589-600, 2007
- [12] S.Geirhofer, L.Tong, B.M.Sadler. "Cognitive Medium Access: Constraining Interference based on Experimental Models". IEEE Journal, Selected Areas Comm. Vol.26 No.1, p.95-105, 2008.
- [13] A.A.El-Saleh, M.Ismail, M.A.M. Ali, A.N.H. Alnuaimy. "Capacity Optimization for Local and Cooperative Spectrum Sensing in Cognitive Radio Networks". Intern. Journal of Electronics, Circuits and Systems, Vol.3, 2009.
- [14] K.Lee, A.Yener. "Throughput Enhancing Cooperative Spectrum Sensing Strategies for Cognitive radios". Proc. of ACSSC, p. 2045-2049, Nov. 2007.
- [15] Y.C. Liang, Y.Zeng, E.Peh, A.T.Hoang. "Sensing-Throughput Tradeoff for Cognitive Radio Networks". IEEE Transaction on Wireless Communication, Vol.7 No.4, p. 1326-1337, 2008
- [16] R.Smallwood and E.Sondik. "The Optimal Control of Partially Observable Markov Processes over Finite Horizon". Operation Research, Vol.21 No.5, p.1071-1088. 1973.

Pre-Filtering In Robust Model Estimation-A Brief Tour

Dalvinder kaur

*Assistant Professor/ Electronics & Instrumentation Department
MD University Rohtak
TITS, Bhiwani, 127021
Haryana, India*

mangaldalvinder@yahoo.com

Lillie Dewan

*Professor/ Electrical Engineering department
NIT, Kurukshetra, 132119
Haryana, India*

I_dewanin@yahoo.com

Abstract

Presence of noise has significant effect on the system identification and parameter estimation. To have accurate system models cleaner data is required which can be obtained if noise is reduced by prefiltering In this paper an attempt has been made to survey the literature on the prefiltering methods in system identification.

Keywords: Pre-filtering 1, Nonarithmatic filters 2, Gaussian noise 3, Moving average 4, Robust H ∞ filtering 5

1. INTRODUCTION

The adaptive ARMA system identification is usually realized by the adaptive equation error and output error algorithm [1], thus, the system identification will be influenced by additive noise caused by various reasons such as disturbance and measurement noise. Measured noise means the measured data invariably contains noise attributed to a no. of causes; sensors and measurement devices, modeled and unmodelled disturbances or unaccounted and unidentified sources. Measurement noise particularly of non – Gaussian type is known to be problematic in identification and parameter estimation and relatively small amount may wreak havoc on linear estimation schemes. Opportunities for improved system identification exist using data prefiltering and noise reducing techniques. In this paper an attempt has been made to study various prefiltering techniques in robust model estimation given in literature. Brief introduction to mathematical model used for identification is given in Section2. Data filtering and three methods form the literature has been discussed in section3 followed by conclusions in section4.

2. MATHEMATICAL FOUNDATION AND PARAMETER ESTIMATION

The autoregressive-moving average (ARMA) model uses present and past inputs with past outputs to determine the present output. The ARMA process is represented by the difference equation

$$Y(n) + a_1 y(n-1) + \dots + a_M y(n-M) = b_0 u(n) + b_1 u(n-1) + \dots + b_K u(n-k) \quad (1)$$

Where a_1, \dots, a_M and b_0, \dots, b_K are called the ARMA parameters. Further information regarding the development of the ARMA model can be found, e.g., in [2, 3, 4]. The ARMA system described by the difference equation (2) can be re-written in the form:

$$y(n) = -\sum_{i=1}^M a_i y(n-i) + \sum_{i=0}^K b_i u(n-i) \quad (2)$$

Compact (2) by writing it in regression model form where the regressor vector is defined by $\varphi(n) = (y(n-1), \dots, y(n-M), u(n), \dots, u(n-K))$

(3)

and the vector parameter by

$$\theta = (-a_1, \dots, -a_M, b_0, b_1, \dots, b_K) \quad (4)$$

(4)

Given (3), (4) and (5) can be expressed as an inner product

$$y(n) = \theta \varphi^T(n) \quad (5)$$

(5)

Note that the parameter vector in (6) is not dependent on n ; therefore, no index is specified for θ in (4) or (5), nor will one be specified in the remainder of this text.

The output-error equivalence method is used to calculate the estimated output and update the parameter estimates. It is achieved by replacing the parameter vector with its time dependent estimate, $\hat{\theta}$ as in

$$\hat{y}(n) = \hat{\theta} \varphi^T(n) \quad (6)$$

Here $\hat{\theta}$ is defined as the most recent parameter vector estimates

$$\hat{\theta} = (-\hat{a}_1, \dots, -\hat{a}_M, \hat{b}_0, \hat{b}_1, \dots, \hat{b}_K) \quad (7)$$

(7)

Subsequently the output estimate (7) can be expressed as

$$\hat{y}(n) = -\sum_{i=1}^M \hat{a}_i y(n-i) + \sum_{i=0}^K \hat{b}_i u(n-i) \quad (8)$$

(8)

The parameter estimates are adjusted incrementally to reduce the error between (5) and (6). The idea is to update the previous parameter values for $\hat{\theta}$ so that the residual error ultimately approaches to zero. This is accomplished using a gradient search technique with a simple quadratic to calculate the error between the models and system outputs.

3. DATA PRE FILTERING

Data pre-filtering is systematically employed in linear identification, mostly for anti aliasing reasons and to reduce the effect of high frequency disturbances in order to increase the signal to noise ratio. It is well known from the linear identification literature [2] that pre filtering may be used to improve model accuracy in a specified frequency band e.g. as a result of control specification which narrow the frequency region over which accurate models are actually needed. In [3] it is pointed out that data prefiltering will introduce bias into the estimates even in the noise free case and a detailed analyses of mean level induced bias is performed. The addition of filters in the identification strategies reduces the impact of noise on parameter estimates.

3.1 Prefiltering using moving average process

IIR prefilter is used in the application of signal frequency estimation [5]. The process of IIR filtering will add extraneous poles to the original signal model and the computational burden is much increased since the estimator order has to be much higher than the order of the estimator

plus the IIR prefilter. FIR prefiltering methods [6] were proposed to increase the signal to noise ratio of original measurement before the singular value decomposition (SVD) based Prony's method was applied to estimate the location of single pose. By FIR prefiltering not only the AR but also the MA coefficient functions are estimated [7]. The optimal moving average coefficients are extracted from the estimated AR coefficients by solving the normal equation SVD and spectral factorization in the frequency domain. Liu and Doraiswami in [8] have emphasized moving average FIR prefiltering. Algorithm given by them is as follow:

3.1.1 Robust estimation of the denominator coefficient

The discrete time domain signal model is assumed to be

$$s(n) = \sum_{i=1}^{M_0} a_i s(n-i) + \sum_{i=0}^K b_i \delta(n-i), \quad l \leq M_0 \tag{9}$$

Where $s(n)$ is the signal, $\{a_i\}$ is the AR coefficient set and $\{b_i\}$ is the MA coefficient set, respectively. $\delta(n)$ is Kronecker delta function. The measurement model is

$$y(n) = s(n) + v(n), \quad 0 \leq n \leq N-1 \tag{10}$$

By using LPCA, the AR coefficients $\{a_i\}$ can be obtained from $y(n)$ in the sense of minimum least squared error. The derivation of standard form LPCA can be found in [7], [8], [9]. LPCA provides high resolution estimates when the signal SNR is high. However its performance degrades severely when the SNR is low.

Let us contact a new signal $\bar{y}(n)$ which is the summing average of the measurement $y(n)$ with data length L , that is

$$\bar{y}(n) = \frac{1}{L} \sum_{i=n}^{n+L-1} y(i) \tag{11}$$

Hence,

$$\bar{y}(z) = F(z)s(z) + F(z)v(z) \tag{12}$$

Where

$$F(z) = \frac{(1 + z + \dots + z^{L-1})}{L}, \quad \text{or} \tag{13}$$

$$F(z) = f_1 + f_2 z + \dots + f_L z^{L-1}$$

In the general case clearly, the $\bar{y}(z)$ and $s(z)$ have the same signal poles location excepting $\bar{y}(z)$ has additional poles due to the measurement noise. Hence, the LPCA can be applied to $\bar{y}(n)$ instead of $y(n)$. The advantage of translating $y(n)$ into $\bar{y}(n)$ is that the strong perturbation of the noise with high level of variance can be greatly reduced if the noise mean η is small (considering the prefiltering be a moving average process) and it is more natural using a linear ARMA model to describe $\bar{y}(n)$ other than the stochastic process $y(n)$ with stronger noise pattern.

3.1.2 Estimation of numerator Coefficients

The estimation procedure of numerator coefficients is also divided into two steps. First, the numerator coefficients of the smoothed measurement $\bar{y}(n)$ are obtained through the similar procedure describe in section II by minimizing the error between $\bar{y}(n)$ and the impulse response $\bar{h}(n)$ generated by the estimated denominator coefficients. Second, the numerator coefficients of the original signal $s(n)$ are calculated by using a squared error minimization and spectral factorization process in the frequency domain.

The ARMA model predictor output of $\bar{y}(n)$ is given by $\bar{y}_{arma}(n) = Z^{-1} \{ \bar{b}(z) / \bar{a}(z) \}$, where

$$\bar{a}(z) = 1 - \sum_{i=1}^M \bar{a}_i z^{-i}, \quad \bar{b}(z) = \sum_{i=0}^M \bar{b}_i z^{-i} \tag{14}$$

$\bar{y}_{arma}(n)$ can be expressed by

$$\bar{y}_{arma}(n) = \sum_{i=0}^M \bar{b}_i \bar{h}(n-i) \tag{15}$$

Where $\bar{h}(n) = Z^{-1} \{ 1 / \bar{a}(z) \}$, that is

$$\bar{h}(n) = \sum_{i=1}^M \bar{a}_i \bar{h}(n-i) + \delta(n), \quad \bar{h}(0) = 1$$

$\delta(n)$ is the Kronecker delta.

Eq. 10 is expressed in the matrix form $\bar{y}_{arma} = \bar{H}\bar{b}$, where $\bar{b} = [\bar{b}_0 \bar{b}_1 \dots \bar{b}_M]^T$, and

$$\hat{Y}_{arma}(n) = \begin{bmatrix} \hat{y}_{arma}(n) \\ \hat{y}_{arma}(n+1) \\ \vdots \\ \hat{y}_{arma}(n+N-1) \end{bmatrix}$$

$$H = \begin{bmatrix} h(n) & h(n-1) & \dots & h(n-M) \\ h(n+1) & h(n) & \dots & h(n-M+1) \\ \vdots & \vdots & \dots & \vdots \\ h(n+N-1) & h(n+N-2) & \dots & h(n+N-M-1) \end{bmatrix} \tag{16}$$

By minimizing $j(\bar{b}) = (\bar{Y} - \bar{H}\bar{b})^T (\bar{Y} - \bar{H}\bar{b})$, where $\bar{Y} = [\bar{y}(n) \bar{y}(n+1) \dots \bar{y}(n+N-1)]^T$. The optimal numerator estimates are obtained from the solution of normal Eq. $\bar{H}^T \bar{H}\bar{b} = \bar{H}^T \bar{Y}$. The above procedure forms an ARMA model estimate of the smoothed measurement $\bar{y}(z)$, or $\bar{s}(z)$ when the mean of $v(n)$ is zero. However, our objective is to obtain the ARMA model parameters of the original signal $s(n)$. The estimate of $s(z)$, namely $\hat{s}(z)$ is calculated from

$$\hat{s}(z) = \frac{\bar{s}(z)}{F(z)}$$

This operation is numerically unstable since in general $F(z)$ will have unstable roots. Hence the estimate of $s(z)$ is obtained from

$$\min \left\| \hat{s}z - \frac{\bar{s}(z)}{F(z)} \right\|$$

Solution of above formula is obtained by spectral factorization which yields

$$\hat{s}(z) = \left(\frac{\bar{s}(z)}{F(z)} \right)$$

Where $(G(z))$, denotes the stable part of $G(z)$.

3.2 Non arithmetic filtering

Applying filters to input and output signals can enhance parameter estimation but may concentrate only on specific frequency bands. Low-, high-, and band-pass filters isolate portions of signals providing opportunities for closer approximations. This technique provides parameter estimates for specific frequency ranges, sacrificing model optimality over the entire operating spectrum. Filters used in this fashion reduce the effects of noise and outliers by obliterating data. Filtering techniques are applied to all of the pertinent signals before parameter estimation is attempted. However, traditional filters used in this manner have the potential to alter the data while attempting to reduce noise and important data can be lost or compromised and introduce new problems.

A class of non arithmetic filters has been developed by the authors [4] and applied to signal smoothing for improved parameter estimation and system identification. This class of filters has been proven successful in reducing induced computational errors such as coefficient quantification and round off. Additionally, this class of filters characteristically eliminates impulsive and Gaussian distributed noise.

The non arithmetic filtering theory employed [4] requires some basic assumptions. It is assumed that data sequences come from a finite totally ordered set (TOS) of values S , and that any subset of data sequence values may be ordered. The sampling rate used in measuring the signals is unspecified and is not restricted to a uniform rate. There exists a distance function (metric) on S which can be user defined. Also, a median-type operator is defined so as to always produce an element residing in S , unlike the usual median operator which may use averaging [10].

The non arithmetic filtering technique demonstrated in [10] evolved as a natural extension of the weighted majority with minimum range (WMMR) filter [4]. The WMMR utilizes a technique of dividing filtering windows into overlapping sub windows in combination with a weighting scheme. The WMMR prefacers' very well, but its highly computational methodology introduces noise in the form of round-off and averaging errors. This consequence led to the development of a nonarithmetic filter. A straight-forward demonstration of the application of nonarithmetic filtering can be obtained using MATLAB System Identification Toolbox [11].

3.3 Robust H_2 and H_∞ Filtering

By using H_2 and H_∞ filtering problem the controller is designed such that worst case induced L_2 gain from process noise to estimation error is minimized. Here an upper bound is tried first and then bound is minimized using techniques based on Riccati equations or LMIs. For a class of uncertain continuous – time systems defined by

$$\begin{bmatrix} \dot{x}(t) \\ y(t) \end{bmatrix} = M(\Delta(t)) \begin{bmatrix} x(t) \\ d(t) \end{bmatrix} \quad (17)$$

Where $x(0) = x_0$, and $M(\Delta(t))$ is given by

$$M(\Delta(t)) = \begin{bmatrix} A & B \\ C & D \end{bmatrix} + \begin{bmatrix} L_1 \\ L_2 \end{bmatrix} \Delta(t) (I - H\Delta(t))^{-1} \begin{bmatrix} R_1 & 0 \end{bmatrix} \quad (18)$$

Where $x(t) \in \mathfrak{R}^n$

Are the states, $d(t) \in \mathfrak{R}^{nd}$ is the process and measurement noise, and $y(t) \in \mathfrak{R}^m$ are the measurements. $A, C, B, D, L_1, L_2, R_1$, and H are known constant matrices with appropriate dimensions. The uncertainty matrix $\Delta(\cdot)$ is norm bounded, time - varying and with problem – specific block – diagonal structure. The set of uncertain matrix values are denoted by

$$\Delta := \left\{ \text{diag} \left(\delta_1 I_{q_1}, \dots, \delta_l I_{q_l}, \Delta_{l+1}, \dots, \Delta_{l+f} \right) : \|\Delta\| \leq 1, \delta_i \in \mathfrak{R}, \Delta_i \in \mathfrak{R}^{q_i \times q_i} \right\} \subset \mathfrak{R}^{n_p \times n_p}.$$

Associated with Δ , define subspaces S and G as

$$S := \left\{ \text{diag} \left(S_1, \dots, S_l, \lambda_{l+1} I_{q_{l+1}} + 1, \dots, \lambda_s I_{q_{l+f}} \right) : S_i = S_i^T \in \mathfrak{R}^{q_i \times q_i}, \lambda_j \in \mathfrak{R} \right\}$$

$$G := \left\{ \text{diag} \left(G_1, \dots, G_l, 0_{q_{l+1}}, \dots, 0_{q_{l+f}} \right) : G_i = -G_i^T \in \mathfrak{R}^{q_i \times q_i} \right\}$$

Note that if $l = 0, f = 1$, then $\Delta = \left\{ \Delta \in \mathfrak{R}^{n_p \times n_p} : \|\Delta\| \leq 1 \right\}$, referred to as *unstructured* uncertainty, denoted Δ_u . In this case, $S = \left\{ \lambda I : \lambda \in \mathfrak{R} \right\}$, and every element of G is 0.

This LFT representation of uncertainty is widely used in robust control theory; for instance, in [12] and [13]. In this note, we assume the representation (17) is well – posed over Δ , meaning that $\det(I - H\Delta) \neq 0$ for all $\Delta \in \Delta$. Under this assumption, the uncertain part can be isolated from known part and the system written as

$$\dot{x}(t) = Ax(t) + Bd(t) + L_1 p(t)$$

$$y(t) = Cx(t) + Dd(t) + L_2 p(t)$$

$$q(t) = R_1 x(t) + Hp(t)$$

$$p(t) = \Delta(t)q(t).$$

$$\Delta(t) \in \Delta$$

Given $L \in \mathfrak{R}^{r \times n}$, the objective is to design a linear, full order filter to estimate $z(t) := Lx(t)$. The filter structure is constrained to: $\dot{\hat{x}}(t) = A_f \hat{x}(t) + B_f y(t), \hat{z}(t) = L_f \hat{x}(t)$, where $A_f \in \mathfrak{R}^{n \times n}$, $B_f \in \mathfrak{R}^{n \times m}$ and $L_f \in \mathfrak{R}^{r \times n}$ are constant matrices. Define estimation error

$$e(t) := z(t) - \hat{z}(t). \text{ Let } \eta(t) := \begin{bmatrix} x(t)^T & \hat{x}(t)^T \end{bmatrix}^T \text{ denote the states of the augmented system}$$

$$\dot{\eta}(t) = \left[\bar{A} + \bar{L}\Delta(t)(I - H\Delta(t))^{-1} \bar{E} \right] \eta(t) + \bar{B}d(t)$$

$$(19)$$

$$e(t) = \bar{C} \eta(t)$$

$$(20)$$

Where

$$\bar{A} = \begin{bmatrix} A & 0 \\ B_f C & A_f \end{bmatrix}, \quad \bar{L} = \begin{bmatrix} L_1 \\ B_f L_2 \end{bmatrix}, \quad \bar{E} = [R_1 \quad 0]$$

$$\bar{B} = \begin{bmatrix} B \\ B_f D \end{bmatrix}, \quad \bar{C} = [L \quad -L_f].$$

In [14], two problems are considered. The H_2 problem (similar to the Kalman filter) has a stochastic interpretation. In (17), assume d is zero mean white noise, with $\mathcal{E}[d(t)d(l)^T] = \delta(t-l)I_{nd}$, where $\delta(t)$ is the Dirac Delta function. The H_2 performance objective is $\sigma := \lim_{T \rightarrow \infty} \sigma_T$, where $\sigma_T = \sup_{\Delta(\cdot) \in \Delta} \mathcal{E} \left\{ (1/T) \int_0^T e^T(t) e(t) dt \right\}$. The notation $\sup_{\Delta(\cdot) \in \Delta}$ denotes the supremum over all piecewise continuous functions $\Delta: \mathfrak{R} \rightarrow \cdot$. The design objective is to minimize σ (by choice of A_f, B_f, L_f) subject to (19) and (20). The H_∞ problem defines the performance measure as $\rho := \sup_{\Delta(\cdot) \in \Delta} \sup \|d\|_2 \neq 0 \left(\|e\|_2 / \|d\|_2 \right)$. (a worst case induced L_2 operator norm). The design objective is to minimize ρ (by choice of A_f, B_f, L_f) subject to (19) and (20).

In [14] it is assumed that (17) is quadratically stable, namely the existence of a positive-definite matrix P such that $A_\Delta^T P + P A_\Delta < 0$ for all $\Delta \in \Delta$. Here, $A_\Delta := A + L_1 \Delta (I - H \Delta)^{-1} R_1$. This is a typical assumption for all work in this area.

4. CONCLUSION

Three main prefiltering techniques to reduce the effects of process noise on parameter estimation have been presented from the literature. A known – arithmetic filtering technique used only input and output data with no a – priori or posteriori system noise information. Where as robust H_2 and H_∞ filters can be used not only for the reduction of the noise but also considers unstructured, non bounded uncertainty case, the upper bounce are directly minimized yielding less conservative results finally one can pose robust filtering as a more general robust control problem, simply used the adhoc iteration methods obtaining adequate results.

5. REFERENCES

1. J.J.Shynk. "Adaptive IIR Filtering". IEEE ASP Magazine, April, 1989.
2. Ljung, L. "Svstem Identification: Theow for the User". T. Kailith ed., New Jersey: Prentice-Hall, 1987.
3. Haykin, S.S. "Adaptive Filter Theory". 2nd ed. Englewood Cliffs, New Jersey: Prentice-Hall, 1991.
4. Longbotham, H.G. and D. Eberly. "Statistical Properties, Fixed Points, and Decomposition with WMMR Filter". JOW of Mathematical Imaging and Vktion: 99- 116,1992.
5. S. Kay. "Accurate frequency estimation at low signal to noise ratio". IEEE Trans. ASSP: 540-547, June 1984.
6. R.Kumaresan and Y. Feng. "FIR prefiltering improves Prony's method". IEEE Tran. Signal Processing, 39 (2): 736-741, March, 1991.
7. R.Kumaresan and D.W.Tufts. "Estimating the parameters of exponentially damped sinusoids and pole zero modelling in noise". IEEE Tran. ASSP, 30: 833- 840, Dec. 1982.
8. R. Doraiswami and W. Liu. "Real-time estimation of the parameters of power system small signal oscillations". IEEE Power Engineering Society IEEEIPES 1992, Winter Meeting, New York, USA, and also to appear in IEEE Trans. on Power Systems.
9. B. Friedlander and B. Porat. "The modified Yula- Walker method of ARMA spectral estimation". IEEE Tran. Aerospace and Electronic Syst., 20:158-173, Mar. 1984.

10. Jack J., Harris and Cheryl B. Schrader. "Application of nonarithmetic filtering techniques for improved system identification". 37th IEEE, Florida USA, Dec. 1998.
11. Ljung, L. User's Guide: MATLAB System Identification Toolbox, The Mathworks, Inc., 1995.
12. L. El Ghaoui and G. Calafiore. "Robust filtering for discrete-time systems with bounded noise and parametric uncertainty". IEEE Trans. Autom. Control, 46 (7): 1084-1089, Jul, 2001.
13. K. Zhou, J.C. Doyle, and K. Glover. "Robust and Optimal control". Upper Saddle River, NJ: Prentice-Hall, 1996.
14. J. C. Geromel, M.C. De oliveira, and J. Bernussou. "Robust filtering of discrete-time linear systems with parameter dependent Lyapunov functions". SIAM J. Control optim.41 (3): 700-711, 2002.

CALL FOR PAPERS

International Journal of Engineering (IJE) is devoted in assimilating publications that document development and research results within the broad spectrum of subfields in the engineering sciences. The journal intends to disseminate knowledge in the various disciplines of the engineering field from theoretical, practical and analytical research to physical implications and theoretical or quantitative discussion intended for both academic and industrial progress.

Our intended audiences comprises of scientists, researchers, mathematicians, practicing engineers, among others working in Engineering and welcome them to exchange and share their expertise in their particular disciplines. We also encourage articles, interdisciplinary in nature. The realm of **International Journal of Engineering (IJE)** extends, but not limited, to the following:

To build its International reputation, we are disseminating the publication information through Google Books, Google Scholar, Directory of Open Access Journals (DOAJ), Open J Gate, ScientificCommons, Docstoc and many more. Our International Editors are working on establishing ISI listing and a good impact factor for IJE.

IJE List of Topics:

The realm of International Journal of Engineering (IJE) extends, but not limited, to the following:

- Aerospace Engineering
- Biomedical Engineering
- Civil & Structural Engineering
- Control Systems Engineering
- Electrical Engineering
- Engineering Mathematics
- Environmental Engineering
- Geotechnical Engineering
- Manufacturing Engineering
- Mechanical Engineering
- Nuclear Engineering
- Petroleum Engineering
- Telecommunications Engineering
- Agricultural Engineering
- Chemical Engineering
- Computer Engineering
- Education Engineering
- Electronic Engineering
- Engineering Science
- Fluid Engineering
- Industrial Engineering
- Materials & Technology Engineering
- Mineral & Mining Engineering
- Optical Engineering
- Robotics & Automation Engineering

IMPORTANT DATES

Volume: 4

Issue: 4

Paper Submission: July 31, 2010

Author Notification: September 01, 2010

Issue Publication: September/October 2010

CALL FOR EDITORS/REVIEWERS

CSC Journals is in process of appointing Editorial Board Members for ***International Journal of Engineering (IJE)***. CSC Journals would like to invite interested candidates to join **IJE** network of professionals/researchers for the positions of Editor-in-Chief, Associate Editor-in-Chief, Editorial Board Members and Reviewers.

The invitation encourages interested professionals to contribute into CSC research network by joining as a part of editorial board members and reviewers for scientific peer-reviewed journals. All journals use an online, electronic submission process. The Editor is responsible for the timely and substantive output of the journal, including the solicitation of manuscripts, supervision of the peer review process and the final selection of articles for publication. Responsibilities also include implementing the journal's editorial policies, maintaining high professional standards for published content, ensuring the integrity of the journal, guiding manuscripts through the review process, overseeing revisions, and planning special issues along with the editorial team.

A complete list of journals can be found at <http://www.cscjournals.org/csc/byjournal.php>. Interested candidates may apply for the following positions through <http://www.cscjournals.org/csc/login.php>.

Please remember that it is through the effort of volunteers such as yourself that CSC Journals continues to grow and flourish. Your help with reviewing the issues written by prospective authors would be very much appreciated.

Feel free to contact us at coordinator@cscjournals.org if you have any queries.

Contact Information

Computer Science Journals Sdn Bhd

M-3-19, Plaza Damas Sri Hartamas
50480, Kuala Lumpur MALAYSIA

Phone: +603 6207 1607

+603 2782 6991

Fax: +603 6207 1697

BRANCH OFFICE 1

Suite 5.04 Level 5, 365 Little Collins Street,
MELBOURNE 3000, Victoria, AUSTRALIA

Fax: +613 8677 1132

BRANCH OFFICE 2

Office no. 8, Saad Arcad, DHA Main Bulevard
Lahore, PAKISTAN

EMAIL SUPPORT

Head CSC Press: coordinator@cscjournals.org

CSC Press: cscpress@cscjournals.org

Info: info@cscjournals.org

COMPUTER SCIENCE JOURNALS SDN BHD
M-3-19, PLAZA DAMAS
SRI HARTAMAS
50480, KUALA LUMPUR
MALAYSIA